Cite as: H. H. Kaplan *et al*., *Science* 10.1126/science.abc3557 (2020).

Bright carbonate veins on asteroid (101955) Bennu: Implications for aqueous alteration history

H. H. Kaplan[1,2]*, D. S. Lauretta[3], A. A. Simon[1], V. E. Hamilton[2], D. N. DellaGiustina[3], D. R. Golish[3], D. C. Reuter[1], C. A. Bennett[3], K. N. Burke[3], H. Campins[4], H. C. Connolly Jr. [5,3], J. P. Dworkin[1], J. P. Emery[6], D. P. Glavin[1], T. D. Glotch[7], R. Hanna[8], K. Ishimaru[3], E. R. Jawin[9], T. J. McCoy[9], N. Porter[3], S. A. Sandford[10], S. Ferrone[11], B. E. Clark[11], J.-Y. Li[12], X.-D. Zou[12], M. G. Daly[13], O. S. Barnouin[14], J. A. Seabrook[13], H. L. Enos[3]

[1]NASA Goddard Space Flight Center, Greenbelt, MD, USA. [2]Southwest Research Institute, Boulder, CO, USA. [3]Lunar and Planetary Laboratory, University of Arizona, Tucson, AZ, USA. [4]Department of Physics, University of Central Florida, Orlando, FL, USA. [5]Department of Geology, School of Earth and Environment, Rowan University, Glassboro, NJ, USA. [6]Department of Astronomy and Planetary Sciences, Northern Arizona University, Flagstaff, AZ, USA. [7]Department of Geosciences, Stony Brook University, Stony Brook, NY, USA. [8]Jackson School of Geosciences, University of Texas, Austin, TX, USA. [9]Smithsonian Institution National Museum of Natural History, Washington, DC, USA. [10]NASA Ames Research Center, Mountain View, CA, USA. [11]Department of Physics and Astronomy, Ithaca College, Ithaca, NY, USA. [12]Planetary Science Institute, Tucson, AZ, USA. [13]Centre for Research in Earth and Space Science, York University, Toronto, Ontario, Canada. [14]John Hopkins University Applied Physics Laboratory, Laurel, MD, USA.

***Corresponding author. E-mail: Email: hannah.kaplan@nasa.gov**

The composition of asteroids and their connection to meteorites provide insight into geologic processes that occurred in the early Solar System. We present spectra of the Nightingale crater region on near-Earth asteroid Bennu with a distinct infrared absorption around 3.4 μm. Corresponding images of boulders show centimeters-thick, roughly meter-long bright veins. We interpret the veins as being composed of carbonates, similar to those found in aqueously altered carbonaceous chondrite meteorites. If the veins on Bennu are carbonates, fluid flow and hydrothermal deposition on Bennu's parent body would have occurred on kilometer scales for thousands to millions of years. This suggests large-scale, open-system hydrothermal alteration of carbonaceous asteroids in the early Solar System.

The Origins, Spectral Interpretation, Resource Identification, and Security–Regolith Explorer (OSIRIS-REx) mission to asteroid (101955) Bennu is designed to return a carbon-rich sample of the asteroid to Earth (*1*). Bennu, a 500-m-diameter near-Earth asteroid, was chosen as the mission target due to its spectral similarity to primitive and organic-rich carbonaceous chondrite meteorites (*2*). Primitive chondritic meteorites formed in the early Solar System so may record the materials, processes, and events that occurred during that period.

The OSIRIS-REx spacecraft entered orbit around Bennu in December 2018. Throughout 2019 and early 2020, the spacecraft acquired images and spectra to characterize Bennu's surface properties, composition, and relationship to meteorites, in advance of sample collection.

Bennu is spectrally classified as a B-type asteroid on the basis of its blue (negative) spectral slope. B-types are a subset of the larger C-complex of primitive asteroids, so-named for their presumably carbonaceous compositions. Bennu's surface contains abundant, widespread hydrated minerals (*3*), widespread magnetite (*3*, *4*), and is dominated by boulders up to ~100 m in longest dimension (*5*). Near-infrared spectra of Bennu's surface exhibit an absorption feature due to hydroxyl in hydrated clay minerals; the band minimum is 2.74 μm, most consistent with hydrated Mg-bearing phyllosilicates (*3*, *6*). Thermal infrared spectra exhibit silicate stretching and bending modes consistent with volumetrically dominant phyllosilicates, as well as absorptions attributable to magnetite near 18 and 29.4 μm (555 and 340 cm^{-1}) (*3*). These observations demonstrate that Bennu is mineralogically similar to the carbonaceous chondrite meteorites that show evidence of water-rock interaction (i.e., aqueous alteration), with the closest meteorite analogs being the most heavily altered members of the CM and CI groups. Aqueous alteration of these meteorites likely took place on a large parent asteroid, >30 km in diameter (*7*), early in Solar System history (*8*). Dynamical analyses suggest that Bennu, a rubble pile asteroid, consists of fragments of a parent body of ~100 km diameter that reaccumulated after a catastrophic disruption (*9*–*11*).

Establishing Bennu's relationship with specific groups of meteorites—whether CI, CM, or others—would provide insight into the geologic processes that Bennu's parent body experienced. The CI and CM groups record diverse scenarios of parent body aqueous alteration. All known CI chondrites are categorized based on their mineral and rock properties as petrologic type 1 (CI1) (*12*). This classifies the CIs as heavily hydrated, and they contain the highest abundances of volatile elements of any meteorites (*13*). CM chondrites span a broader range of degrees of aqueous alteration, from petrologic type 1 to 2 (*14*, *15*). The CM chondrites are depleted in volatiles relative to the CIs. Although the CM1 and CI1

meteorites are both highly aqueously altered, they have distinct bulk chemistry and textures (*15*). There are other carbonaceous chondrites that cannot be classified into any of the known groups and are therefore termed "ungrouped" (*16*). Grouping chondrites together implies that they likely originate from the same geologic context; if a carbonaceous chondrite is ungrouped, it is possible that it has a distinct geologic origin. We consider recent observations of asteroid Bennu within this meteorite framework, to constrain its geologic history and make predictions for the sample that will be returned to Earth.

Spectra of carbon species on Bennu

In global observations of Bennu collected during the Detailed Survey–Equatorial Stations campaign of the OSIRIS-REx mission (25 April to 6 June 2019) (*1*), the OSIRIS-REx Visible and InfraRed Spectrometer (OVIRS) (*17*) detected a ubiquitous infrared absorption feature near 3.4 μm (*18*), a spectral region associated with carbon-bearing species. OVIRS measures reflected light at wavelengths from 0.4 to 4.3 μm with a circular, 4-mrad field of view (*17*). Between 3.2 and 3.6 μm, there are at least five absorption minima attributed to organic molecules, including symmetric and asymmetric stretching modes of methyl (–CH_3) and methylene (–CH_2) groups (i.e., aliphatic CH), and an aromatic CH stretch. Carbonates have overlapping absorption features in this wavelength region from overtones (absorptions occurring at higher-energy multiples of the fundamental frequency) and combinations of the fundamental stretches in CO_3.

The global data have a spatial resolution of ~30 m in the direction of spacecraft motion (along-track) and 20 m in the perpendicular direction (cross-track), with coverage of nearly the entire asteroid surface (*18*). The complex spectral features near 3.4 μm in this dataset are attributed at the global scale to mixtures of organics and carbonates (*18*). The spectral shape in this wavelength region is repeatable to <1% across multiple observations of the same surface spot, indicating that instrumental and illumination effects do not cause the observed absorption complexity (*18*).

We analyzed higher-spatial-resolution OVIRS observations that were collected in October 2019 during the first Reconnaissance (Recon A) phase of the OSIRIS-REx mission, which entailed more detailed investigations of candidate sampling sites. We used data from the region around Nightingale crater, the mission's primary sampling site to provide context for the sample return. These observations have spatial resolutions of ~4 m cross-track and 9 m along-track for each OVIRS footprint.

The 3.4-μm feature has different shapes in the Nightingale observations from those in the global observations (*18*), indicating that it may be possible to distinguish compositions at higher spatial resolution. To discriminate between organics and carbonates, we use a chi-square goodness of fit test, band minima positions, and visual inspection (*19*). The goodness of fit test uses a set of 220 laboratory spectra of carbonates and organics with a range of compositions to assess how closely these laboratory data match the shape of the OVIRS data (table S1). Uncertainties were determined by adding noise to the laboratory spectra to mimic the OVIRS signal-to-noise ratio (SNR) near 3.4 μm (*19*). We find that chi-square values of < 1 can identify either carbonate minerals or organics with >99% confidence (>95% confidence for chi-square < 2) (table S1).

Organic and carbonate spectral features differ in terms of number of minima, minima positions, and absorption widths. We identify some OVIRS spectra with 3.4-μm features that are consistent with carbonates and others that are consistent with organics (Figs. 1 and 2). The OVIRS spectral shapes consistent with organics are similar to those previously detected near 3.4 μm in asteroids (e.g., (*20*–*22*)) and meteorites (*23*) (Fig. 2). These features have a narrow minimum at 3.42 μm or a broad, flat feature centered at 3.42 μm (e.g., (*24*)). The OVIRS spectral signature consistent with carbonates is primarily identified by an absorption feature with two minima near 3.4 μm (Fig. 1). The band positions vary by tens of nanometers, consistent with known changes in wavelength of carbonate absorptions with varying cation composition (Fig. 3). The OVIRS spectra that are best fitted with carbonate laboratory spectra (Fig. 2) are poorly fitted with organic laboratory spectra (fig. S1).

The carbonate-matching OVIRS spectra include features similar to calcite ($CaCO_3$), siderite ($FeCO_3$), magnesite ($MgCO_3$), dolomite ($CaMg(CO_3)_2$), and/or breunnerite ($(Mg,Fe,Mn)CO_3$) (Fig. 1, 2). We cannot distinguish calcite and siderite at the spectral resolution and SNR of the OVIRS data near 3.4 μm; however, Fe in siderite would produce a broad absorption near 1 μm, which is not detected (fig. S2). Siderite is rare in carbonaceous chondrite meteorites, whereas calcite is abundant (*24*). We therefore conclude that calcite is the most likely carrier responsible for these carbonate-matching spectra. Aragonite has the same composition as calcite ($CaCO_3$) with a different crystal structure; it has similar spectral properties to calcite at wavelengths < 2.5 μm (*25*), but appropriate laboratory spectra are not available, so it is not included in our analysis. Spectra we identify as dolomite could alternatively be due to Fe-rich breunnerite, which has an absorption feature at a similar wavelength. For more Mg-rich forms of breunnerite, we expect the band position to shift toward shorter wavelengths, similar to magnesite. We have not found a 3.4-μm feature on Bennu that corresponds to natrite (Na_2CO_3), which was detected in the brightest regions of dwarf planet Ceres and has minima at longer wavelengths than calcite (*26*).

In addition to the feature at 3.4 μm, carbonates are expected to produce an absorption near 4 μm. OVIRS has an

SNR of 50 at 3.4 μm, but signal decreases rapidly beyond ~3.6 μm, with SNR of only 15 at 4 μm. Low SNR reduces our ability to detect the expected carbonate absorption near 4 μm, but we do find a possible absorption feature in this region that is correlated with the 3.4-μm feature (fig. S2). Overtones at ~2.35 and, possibly, 2.55 μm are also observed in the OVIRS spectrum (fig. S2) and may be due to carbonate and/or Mg/Fe phyllosilicates. However, these features have <2% band depth, the strength of the absorption feature compared to the continuum, and any variation in band depth is within the uncertainty.

Thermal infrared spectra from the OSIRIS-REx Thermal Emission Spectrometer (OTES) (*27*) exhibit a spectral feature near 7.04 μm (1420 cm^{-1}) that may be attributable to carbonates (*28*), but this feature has not been definitively assigned (*3*). Another carbonate feature, the ν_3 (third fundamental) absorption, is expected at ~6.35 to 6.75 μm (1500 cm^{-1}) and has been observed in laboratory and remote sensing data (*28*, *29*); however, it has not been identified in OTES global spectral observations (spatial resolutions of 20 to 40 m). Nor have other expected carbonate features, including the narrow, ν_2 fundamental absorption near 11.3 μm (886 cm^{-1}) and a large, broad, fundamental absorption between ~25 and 33 μm (~400 to 300 cm^{-1}). Detection of spectral features in the thermal infrared depends on SNR, temperature, physical conditions (e.g., roughness or cavities), phase abundance, the compositions of the other phases that are present, spectral resolution, and particle size (*19*). These factors may explain the non-detection of these carbonate bands, despite the higher SNR of the OTES data relative to that of the OVIRS data.

We mapped a ~0.03-km^2 area surrounding the Nightingale sample site (~56.04° latitude, 42.05° longitude), within which ~1% of the 3396 OVIRS spectra have a chi-square < 1 match to laboratory spectra of carbonates, rather than organics or mixtures, and ~15% have chi-square < 2 (Fig. 2) (*19*). Organics account for <1% (chi-square < 1) or 8% (chi-square < 2) of the spectra based on these goodness of fit tests. The spectral signatures with chi-square < 1 match to carbonates are strongest at the rim of Nightingale crater and on individual boulders in the area. Some of these same surface features are also associated with the strongest absorptions at 3.2 to 3.6 μm, though many are not (Fig. 4). The majority (~64%) of the carbonate signatures have band positions that are consistent with calcite, followed by magnesite/Mg-rich breunnerite (~24%) and dolomite/Fe-rich breunnerite (12%) (Figs. 2 and 3).

Bright vein-like features and mottling in boulders

To provide geologic context for the spectral observations, we examined high-resolution (~1.4 cm $pixel^{-1}$) images of the Nightingale region acquired by the OSIRIS-REx Camera Suite (OCAMS) PolyCam imager (*30*, *31*) during Recon A. We found centimeter- to meter-scale features on boulders that are distinctly brighter than the surrounding host rock. Some of these features are elongated and linear, whereas others are irregularly shaped. They are apparent in the raw camera images, with digital number (DN) values between 1.4 and 1.9× the average value of the host rock (table S3), indicating higher reflectance than the average Bennu surface.

To quantify the brightness and morphology of these features, we focused on three host boulders (Fig. 5). We radiometrically calibrated the images using the mission's standard calibration process (*31*). This process converts raw DN values to reflectance (also known as radiance factor or *I/F*), the ratio of incident solar radiation that is reflected from the asteroid to that which would be reflected from an ideal Lambertian surface normally illuminated by the Sun. The reflectance values are then used to determine the bright material's normal albedo, defined as the reflectance at normal observing conditions (0° solar incidence, 0° solar phase, and 0° emission angles). We registered the calibrated images to digital terrain models (DTMs) of the boulders, previously produced from OSIRIS-REx Laser Altimeter (OLA) data with an average facet size of ~7 cm (*19*, *32*). We estimated the observed photometric angles by ray tracing from the registered position and orientation of the camera to the DTMs. We used the derived angles as inputs to the Robotic Lunar Observatory photometric correction (*33*) to compensate for the reflectance variations resulting from changing viewing and illumination conditions. We then measured the absolute difference in normal albedo between the bright features and their host rocks.

The median normal albedo of Bennu, ~4.4%, is among the lowest of any object in the Solar System (*5*, *34*). Analyses of the photometrically corrected images show that the bright features have normal albedos of at least 10 to 19% (Fig. 5; table S3). The mean normal albedo of the host boulders varies between 6.0 and 7.6% (table S3), which is also brighter than Bennu's global average.

We performed further analysis of one of the bright feature–bearing boulders (labeled VBR-13 in Fig. 5, where VBR stands for vein-bearing rock) to assess the uncertainty and variability of the derived normal albedo values. This boulder was identified in 13 images taken at varying resolutions and observation geometries (table S3). In images with pixel scales ranging from 1.3 to 4.8 cm $pixel^{-1}$, the normal albedo of the bright material ranges from 14 to 19% (±2.2%, 1σ) (table S3). We rule out textural and observation geometry effects and conclude that the bright features are high-reflectance material included in the host rocks.

The three illustrative examples of the elongated, linear bright features are 3 to 15 cm thick and vary in length from 50 to 150 cm, though smaller examples exist (Fig. 6). These occur at sharp edges of boulders so may be small exposures

of a larger internal layer. We interpret all these features as veins—narrow, linear features formed when an aqueous solution flows through a rock, depositing minerals by precipitation, usually within pre-existing fractures. Shock processes can also create linear or planar features, and melt veins created by shock events are found in some meteorites (*35*). Shock melt veins are darker than the surrounding meteorite matrix, whereas the veins on Bennu are brighter than their host rocks.

The irregularly shaped bright features in darker host rocks produce a mottled appearance (Fig. 6). Similar mottled boulders occur on another C-complex asteroid, (162173) Ryugu (*36*). The irregular features on Bennu are typically >10 cm in the longest dimension, range from angular to rounded, and can occur individually or in clusters.

The host rocks of the veins and irregular features span a range of albedos and sizes but tend to have similar morphologies. The host boulders appear to be part of a previously identified population that has a distinct, brighter albedo distribution (though not as bright as the veins and irregular features they host) relative to the dark boulders that dominate Bennu's surface, and a more negative spectral slope at ultraviolet (UV) wavelengths (*37*). These brighter boulders also have a different texture, appearing smoother and more angular than the dark boulders on Bennu. The former exhibit fractures and pits and appear to be harder and less easily broken down than the other, more hummocky observed boulder morphologies. The largest bright boulder is ~10 to 12 m; all of the largest boulders ($\gtrsim$ 20 m) on the asteroid are dark (*5*). In many cases, boulders that host bright veins or irregular features do so only on a single face. A few small boulders have bright material that dominates an entire face (fig. S3). Analysis of their colors is published elsewhere (*37*). They have higher thermal inertias than the dark boulders, which may indicate lower porosity (*38*), as we expect for precipitation of vein-filling materials in fractures and void spaces.

Carbonates and veins in meteorites

Although meteorites are a biased sample of the asteroids from which they are derived, comparison may offer insight into the possible carbonate mineralogy and vein-filling materials on Bennu. We therefore searched previously published studies for evidence of carbonate minerals and bright veins in the carbonaceous chondrite meteorites.

The carbonate mineralogy of carbonaceous chondrites is a function of their alteration history. CM chondrites contain on average <4 vol.% carbonate (*39*–*41*). The least altered CM chondrites contain calcite as the dominant carbonate mineral (*39*, *42*). With increasing degrees of alteration, dolomite appears, followed by breunnerite (*42*–*44*). In the most altered samples, dolomite, breunnerite, and calcite are replaced (in that order) by Fe-rich serpentine, Fe–Ni sulfides, and Mg-rich serpentine (*39*). In CM chondrites of all sub-types, a second generation of calcite forms after the sulfides and phyllosilicates by replacement of remaining anhydrous silicates and dolomite (*39*).

The carbonate mineralogy of the CI chondrites is similar to that of the most altered CMs. CI meteorites contain four types of carbonates (dolomite, breunnerite, calcite, and siderite) comprising an average of 5 vol.% of the samples (*24*). However, the abundance of carbonates in some individual lithic fragments of CIs exceeds 10 vol.%. A lithic fragment in Ivuna (a CI) has calcite as the only carbonate, which accounts for more than 20 vol.% (*24*). Another clast has 21.5 vol.% carbonate (*45*). A dark matrix clast in Orgueil, another CI, contains ~35 vol.% of pure calcite (*46*). CIs have greater diversity in carbonate cations than CMs, including more Mg in breunnerite and magnesite. In CIs, dolomite is the most abundant carbonate phase, with breunnerite and calcite being much less abundant (*24*, *44*, *47*). Siderite is extremely rare, with only one grain reported (*24*).

Similar to the highly altered CMs and the CIs, the ungrouped carbonaceous chondrite Tagish Lake has a carbonate-rich lithology with calcite, dolomite, and Fe- and Mg-rich breunnerite spread diffusely through the matrix (*48*). The CR chondrites also have carbonates up to 5.7 vol.% (*49*).

Most carbonates in CI and CM chondrites occur as grains 10 to 50 μm in diameter distributed throughout the matrix. However, carbonates in some carbonaceous chondrites occur as veins or vein fragments (*39*, *50*). For instance, the CM chondrite SCO 06043 is crosscut by dolomite veins hundreds of microns in length (*39*). LON 94101, another CM chondrite, contains calcite that occurs as millimeter-sized veins (*50*). Carbonate aggregates (~100 μm across) resembling fracture fillings have been observed in the Orgueil and Alais CI chondrites (*24*, *51*). These have been interpreted as vein fragments that were mechanically disrupted and dispersed during breakup of the host rock (*24*). Veins up to ~300 μm in length are observed in Belgica 7904, a chondrite with similarities to both the CI and CM groups (*52*). Veins of carbonates also occur in some CR chondrites, such as in Renazzo and GRO 95577 (*40*, *53*).

Other vein-filling minerals are found in meteorites. Fractures ≤500 μm long are filled with smectite-chlorite in the ungrouped carbonaceous chondrite Y-82162 (*54*). Phyllosilicate–magnetite structures and 'trains' of magnetite crystals in Orgueil have been interpreted as recrystallized veins (*55*). Sulfate and phyllosilicate veins occur in some CIs (*44*), and sulfate and Fe-rich veins are found in CMs (*56*). At least some of the sulfate veins are thought to be terrestrial weathering products (*57*).

The presence of bright, carbonate-filled veins in meteorites suggests a connection between our observations of carbonate-matching spectra and bright veins in the Nightingale

area. The carbonate compositions that best match the spectral signatures on Bennu are similar to those of the CI chondrites and the most aqueously altered CM chondrites (*24*, *39*, *43*, *58*), which are sometimes expressed as veins.

Composition of veins on Bennu

In addition to the spectral evidence indicative of carbonates (calcite, magnesite, dolomite, and breunnerite) that we present, known phases on Bennu's surface include Mg-rich phyllosilicates (*3*), the Fe-oxide magnetite (*3*, *4*), aliphatic organic molecules (*18*), and a few pyroxene-rich boulders likely originating from the Vesta asteroid family and delivered by impact (*59*). We consider whether any of these other phases could be potential vein-filling minerals.

Phyllosilicate veins in meteorites have similar compositions to their host rock (*54*) and therefore are unlikely to have distinct albedos from their surroundings, which is inconsistent with the bright veins and irregular features that we observe in host boulders. The exogenous pyroxene-bearing boulders have brighter normal albedos of ~10 to at least 26% (*59*). However, they have distinctive spectral features in the 1- and 2-μm region that we do not observe in OVIRS spectra covering the bright features. Sulfates are present in Bennu-analog meteorites, but the signatures observed in meteorite spectra (i.e., Ca-sulfate: distinctive features at ~1.4, 1.75, 1.9, and 2.1 to 2.2 μm) (*60*) are not detected in the OVIRS spectra. Magnetite and organics are optically opaque and unlikely to have the normal albedos of 10 to at least 19% observed for the bright features and veins (*23*, *61*). Thus, although the 3.4-μm feature in some OVIRS spectra could be attributable to organics rather than carbonates (Fig. 2), the low albedo of organic-rich material means that it is not a plausible candidate for the dominant composition of bright veins on Bennu.

We conclude that carbonate is the most likely bright vein-filling material. Magnetite, sulfides, and organic phases may also be present in smaller abundances. These phases are commonly associated with carbonates in carbonaceous chondrites (*45*). Pure carbonates have albedos approaching 100% (*62*), but minor abundances of opaque minerals (e.g., magnetite and sulfides) can reduce albedo to the level of the bright features on Bennu (*63*). Coarser grain size can also reduce albedo (*64*).

Reciprocally, the bright veins and irregular high-reflectance features in boulders on Bennu are the most likely source of the carbonate-matching spectral signatures that we detected in the higher-spatial-resolution OVIRS data. Hereafter we refer to these 3.4-μm spectral signatures as carbonate signatures.

However, even at the highest spatial resolution available, OVIRS footprints are too large to isolate individual bright features. For instance, the veins in Fig. 6 only account for <0.1% of an OVIRS footprint (~28 m^2), and their host boulders account for 7 to 35% of a footprint. Previous work has shown that OVIRS is highly sensitive to bright material, even in cases where it accounts for <1% of the instrument field of view (*59*). Changes in viewing geometries and outcroppings could block carbonate from the view of the spectrometer, explaining the variable strength of the carbonate feature in the spectral data (fig. S4).

We used a linear mixture analysis to assess whether carbonates, sequestered in veins comprising <0.1% of an OVIRS footprint, could account for the spectral signatures we observe (*19*). We found that very small fractions of carbonate, typically <0.5%, are enough to reproduce the features seen in the OVIRS spectrum (Fig. 6).

Near the Nightingale site, most of the OVIRS spots that cover veins (Fig. 6) have a calcite signature, which is the most common carbonate spectral signature on Bennu (Fig. 2, 3). Signatures that may indicate more Mg-rich carbonates (dolomite, magnesite, breunnerite) are commonly associated with larger, bright boulders (up to ~10 m), sometimes without visible evidence for veins or mottling (Fig. 4). Some areas have carbonate signatures with no visible veins or bright irregular features, but where small boulders consistent with the vein-hosting type are present. We attribute these detections not associated with a visible feature to more diffuse carbonate material, as would be expected in boulders or regolith where carbonate deposition may have occurred in micropores or fine veinlets, veins may have been brecciated and dispersed through impact gardening, or carbonates may have formed by fine-scale alteration processes that did not cause development of veins. It is also plausible that there is visible-scale carbonate-rich material within a host rock that is simply not exposed on the boulder face (e.g., VBR-14 in Fig. 5).

Conversely, we observe some veins in OVIRS spots without a strong carbonate signature. These spots tend to have spectral signatures of organics or organic-carbonate mixtures, which could indicate that a greater proportion of organics is present that is obscuring the carbonate signature, or that viewing geometry effects are depressing the carbonate band depth (fig. S5) (*19*).

Carbonate abundances on Bennu

Though carbonaceous chondrites contain carbonate, they rarely show spectral evidence of it in the visible–near-infrared (VIS-NIR) wavelengths covered by OVIRS (0.4 to 4.3 μm). Carbonaceous chondrites with some of the highest carbonate abundances exhibit a 4-μm carbonate absorption (e.g., Tagish Lake, (*23*)), but evidence of carbonate in the region from 3.2 to 3.6 μm is rarely found in meteorite spectra. Among published carbonaceous chondrite spectra, <2% have evidence for carbonate in this spectral region, with most either having no absorption or an organic absorption feature (table S4). There are no known organic-carbonate mixtures in

carbonaceous chondrite spectra, suggesting that the abundances and/or spectral mixing regime on Bennu are distinct from that in the meteorites. Outcroppings of carbonate in meter-length veins could produce such a distinct spectral mixing regime, which would not be represented in meteorites.

Because carbonate has not been definitively detected in OTES spectra, we can place constraints on its abundance. For particles that are larger than the wavelength of light, thermal infrared spectra are the linear sum of the spectral signatures of all component phases in proportion to their abundance (*65*). Typically, such data are sensitive to individual phases at volumetric abundances of a few percent or more in laboratory and remote sensing mixtures (*66*). The absence of these features suggests that, at global to regional scales, carbonate is unlikely to constitute more than a few percent of Bennu's surface mineralogy. At local scales (single to a few spectra), OTES's SNR is low at wavelengths less than ~7.4 μm, making detection of the ν_3 fundamental band challenging. At longer wavelengths, there are no substantial differences from global and regional averages in the features near 11.3 and 25 to 33 μm. This is consistent with absolute abundances of a few percent or less at the scales of most OTES global observations.

If carbonate is concentrated in the veins and irregular bright features on Bennu, it would account for only a percent or less of the area of each OVIRS spot, or 0.5% of an OTES spot (fig. S6). Such an abundance is consistent with the lack of OTES detection and with our linear mixture analysis, which indicates that only a fraction of a percent of the surface needs to be carbonate to account for the OVIRS signatures (Fig. 6). OVIRS may be particularly sensitive to carbonates if they are segregated from other surface materials and bright compared to their surroundings, as is the case for the pyroxene-bearing boulders (*59*). Although outcroppings of carbonate at the scales of veins observed on Bennu are not represented in the meteorite collection, the overall abundances of carbonate on Bennu may be similar to those of the meteorites (a few vol.% or less). The clasts with high vol.% carbonate found in some CI chondrites could result from the breakup of larger features by impact. We expect high concentrations of carbonate in meteorites if centimeter- and meter-scale carbonate features are present on their parent bodies.

Hydrothermal alteration on Bennu's parent body

Distance

Uninterrupted veins up to 150 cm long, such as those that we observe in the OCAMS data, are too large to have formed on Bennu itself and thus must have survived from the parent body. We interpret these veins as most likely originating in the same aqueous system that is responsible for the overall level of hydration observed on Bennu.

Models of carbonaceous asteroid thermal evolution, based on meteoritic evidence, indicate that aqueous alteration was driven by hydrothermal convection (e.g., (*67*)). It is unclear whether aqueous alteration occurred in a chemically closed system, in which bulk chemistry did not vary on the length scales of the meteorites, or an open system in which fluid flow promoted chemical fractionation (*50*). The unfractionated bulk chemical compositions of the carbonaceous chondrites appear incompatible with fluid flow over the large distances expected for open systems (*13*, *68*, *69*). Closed-system models are consistent with carbonaceous chondrite unfractionated bulk chemical compositions and their oxygen isotopes (*14*, *47*, *67*, *70*, *71*). The latter models are supported by the low permeability of parent body interiors (*72*). Open-system hydrothermal alteration scenarios suggest that fluids flowed through fractures from the interior to the exterior of the asteroid, and carbonate minerals precipitated into these fractures as veins (*24*). Oxygen isotope evidence has been alternatively interpreted as indicative of such open systems with large-scale fluid flow (*73*, *74*). Numerical simulations of parent body evolution also suggest asteroid-scale fluid mobility (*75*–*78*).

The putative carbonate veins that we observe on Bennu are orders of magnitude larger than any known in meteorites. We used mass balance constraints to estimate the size of the hydrothermal systems required to produce the observed veins on Bennu. Assuming that the veins are pure calcite, they would contain 56 weight% CaO; this is an upper limit, given the lower albedo of the veins relative to pure carbonate. Previous analysis showed that the bulk abundance of CaO in Orgueil, which has major element abundances similar to the solar photosphere and hence the bulk Solar System, is 1.36 weight%, of which 0.63 weight% is soluble (*46*). Thus, formation of calcite veins requires a rock volume 41× that of the vein, if all of the Ca is removed from an Orgueil-like host rock. If only the soluble component is mobilized, then the alteration volume increases to 89× that of the vein. The largest observed vein on Bennu is 14 cm thick. This thickness implies that a volume of host rock extending between 288 and 622 cm above and below the vein must have been leached of Ca, if carbonate fills the vein. Thus, hydrothermal alteration on Bennu would have occurred on the scale of at least meters. However, this estimate is a lower limit as it requires substantial elemental fractionation of nearby host rocks, which is inconsistent with bulk chondritic elemental abundances.

Carbonate formation during aqueous alteration in CM chondrites would have occurred at moderate temperatures (<35°C) and pressures (<10 MPa) in the interior of a parent asteroid (*69*). These conditions are consistent with experiments of calcite vein formation performed at temperatures of 22–23°C and ambient atmospheric pressure (~100 kPa) (*79*). These experiments indicated that a large volume of fluid is required to produce calcite veins: typically, a fluid/calcite volume ratio of 10^5 to 10^6 for formation of thin short veins. Applying these values to the thickest veins on Bennu suggests

fluid flow at the scale of 20 to 45 km on either side of the vein, implying a nearly global, open hydrologic system on Bennu's ~100-km-diameter parent body (*11*, *19*).

Our calculations support the open-system model of asteroidal aqueous alteration. In this scenario, internal pressurization drove fluid flow from the interior of Bennu's parent asteroid through pore spaces to the asteroid surface, where water could be lost into space. As water ice melted, liquid water migrated through high-permeability fractures created by impact-induced brecciation (*24*, *39*, *50*, *58*, *80*). Alternatively, crack propagation could have been driven by over-pressurization of gas formed during alteration (*81*). The reactants Ca and CO_2 were leached from host rock and transported over distances of meters to kilometers. As the hydrothermal solution cooled, calcite crystals grew into open pore spaces along the fractures, forming the veins we observe on Bennu. This mechanism is consistent with calcite in CM chondrites having formed by cementation of fluid-filled fractures (*50*, *58*).

Impact processing of the parent asteroid regolith could have continued after vein formation. The catastrophic disruption of the parent body and re-accumulation of rubble to form Bennu likely fractured rocks along the weak carbonate veins, potentially explaining why they are sometimes exposed on apparently broken faces. Thus, the geologic expression of the veins on Bennu has been modified by its violent history.

Time

Aqueous alteration likely proceeded progressively in multiple phases or events. Several episodes of alteration occurred on the CI parent body (*24*). Coexisting calcites and dolomites in CM chondrites are not in equilibrium so also formed in distinct events (*44*, *80*). Dolomites typically form slightly earlier than breunnerites. Extensive aqueous activity on the Orgueil parent body occurred over a period of several million years, starting ~3 to 4 Ma after formation of the Solar System (*82*). The probable difference in age between dolomite and breunnerite indicates temporal variations in fluid composition (*82*). Different carbonates (e.g., calcite, dolomite, and breunnerite) are characterized by distinct oxygen and carbon isotopic compositions (e.g., (*83*)). Much of the calcite in CM chondrites represents a second generation that formed after the first-stage alteration that established the dominant phyllosilicate mineralogy (e.g., (*39*)). This scenario is consistent with our observations of bright, ostensibly calcite veins hosted in fractures in phyllosilicate-rich boulders.

Carbonate precipitation timescales depend on factors such as fluid saturation state, flow velocity, vein dimension, and kinetic rate constants and reaction order. We apply a kinetic model (*79*) to constrain the time necessary for vein filling, finding that the veins on Bennu developed on the parent body over thousands to millions of years (*19*).

These timescales are consistent with the timing of crystallization indicated by Mn-Cr dating of carbonates in CI and CM chondrites. Calcites and dolomites in four CM chondrites all have formation ages of $3.8^{+0.4}_{-0.5}$ Myr after the formation of the oldest Solar System solids (*84*). The crystallization ages of dolomite in the QUE 93005 and Sutter's Mill carbonaceous chondrites indicate that aqueous alteration occurred at a similar timing of 3.93 ± 0.23 Myr (*42*) and 2.4–5.0 Myr after the birth of the Solar System (*85*), respectively.

Does Bennu have a meteorite analog?

Spectral data from OVIRS and OTES collected while approaching the asteroid indicated that Bennu's mineralogy and chemistry were consistent with the most aqueously altered CM chondrites but did not rule out the presence of some CI-like material (*3*). We build on that analysis with the spectral and geologic features we observe at Nightingale to further constrain Bennu's relationship to the carbonaceous chondrite meteorites.

Bennu's observed global spectral properties are broadly consistent with a highly altered CM chondrite mineralogy (e.g., CM1): Bennu has a hydration band minimum at 2.74 μm, a position that is associated primarily with Mg-serpentine (e.g., antigorite) but could incorporate some Fe-serpentine (cronstedtite) (*3*). The CIs, however, have band minima at shorter wavelengths (2.71 μm) associated with the phyllosilicates saponite and Mg-serpentine (lizardite and chrysotile) (*6*). The OTES data suggest that Bennu's surface is dominated by phyllosilicates, consistent with the most aqueously altered CMs (*3*).

Though calcite is the most common carbonate mineral that we identify on Bennu, at least one-quarter of the carbonate detections are more Mg-rich compositions based on the wavelength of their 3.4-μm features (Fig. 3), including likely dolomite, breunnerite, and magnesite. Only calcite, breunnerite, and dolomite have been found in CM chondrites, possibly because Mg is limited to dissolution from olivine, which occurs in only the most altered CMs (*39*, *43*). Magnesite has only been reported in the CIs (*47*, *86*) and in some ungrouped carbonaceous chondrites (*87*), so the presence of magnesite on Bennu could imply a closer relationship to these meteorites. However, calcites still account for the largest individual fragments in the CIs (*46*), and vein-filling calcites are found in both CIs and CMs (*24*, *39*, *51*).

CM and CI meteorites are usually assumed to originate from different asteroid parent bodies. The bright veins and irregular features on Bennu are associated with a specific boulder morphology and reflectance range, so could have a different composition, and thus a distinct source, from the other boulders on Bennu. However, though the vein-bearing boulders belong to a population with distinctive albedo and color (*37*), there is no indication that the hydration band

minimum position or depth for these boulders is different from that of the rest of Bennu (*18*), though much of the spectral data have a spatial resolution too low to isolate individual boulders of this type. Bennu's rubble-pile structure and diverse boulder morphologies are consistent with a mixture of compositions from multiple locations within its parent asteroid.

Bennu may bear the closest resemblance to the ungrouped carbonaceous chondrite meteorites with similarities to both CMs and CIs. For instance, the ungrouped carbonaceous chondrite Tagish Lake has mineralogy, oxygen isotope, and bulk chemical composition that fall between those of the CMs and CIs (*88*). It has a carbonate-rich lithology that contains both calcite and Fe,Mg-carbonates intermixed with saponite and magnetite clasts (*88*). Tagish Lake is dynamically and spectrally linked to outer main belt C-complex asteroids with red spectral slopes (*89*), so we do not suggest that it is directly related to the blue-sloped Bennu. However, Bennu may similarly represent an ungrouped, intermediate composition of chondritic material. The bright centimeter-scale irregular features and meter-scale veins on Bennu, which are also not represented in meteorites, may be characteristic of this particular material; alternatively, it may be common on carbonaceous chondrite parent bodies but only observed on Bennu, where we are able to make observations at the outcrop scale. Mottled boulders on Ryugu could be a similar expression of bright, carbonate-bearing material; however, this cannot be confirmed with the spectrometer on Hayabusa2, which does not cover the 3.4-μm region.

Vein fragments in carbonaceous chondrites could be rare because most carbonate veins have been broken up and scattered by impacts (*44*, *51*). Carbonate veins may be preferentially destroyed by the ejection process and/or passage through Earth's atmosphere, reducing the likelihood of being represented in the meteorite record. Meteorite collection parties might not recognize carbonate-rich fragments as possible meteorites.

Role of space weathering

Space weathering can modify the spectrum of an exposed surface, complicating comparison between in situ spectra of Bennu and the interiors of meteorites. The influence of space weathering on Bennu's spectral properties is only partly understood. The bright boulder population that hosts the veins and irregular features appears more resistant to space weathering than dark boulders on Bennu (*37*). Irradiation experiments performed on meteorites indicate that a wide range of changes in VIS-NIR spectral slope are possible (*90*). Space weathering can destroy aliphatic organics (*91*), which could explain the variable organic and carbonate mixture signatures that we observe with OVIRS. In this scenario, more recently exposed surfaces would have stronger organic absorptions that weaken with time. Bennu is known to eject particles from its surface; the mechanism is unknown but could expose material from the interior (*92*). The spectral signature of carbonate and mixtures, where present, still implies either an unexpectedly high abundance or, more likely, an unusual outcropping of carbonate, compared to the carbonaceous chondrite spectra.

OSIRIS-REx's sampling mechanism is designed to collect the top several centimeters of Bennu's regolith (*93*), whereas the spectrometers only measure the top tens to hundreds of microns. Thus, space-weathered material may be in the minority of the collected sample, unless regolith mixes on the centimeter scale on timescales longer than the rate of space weathering. Material attached to the spacecraft's surface contact pads could distinguish surface-exposed material from un–space-weathered material in the near subsurface.

Thermal evolution and organics

Most aqueous alteration in the CIs and CMs occurred at temperatures <150°C, but some meteorites have experienced additional heating to higher temperatures (*86*). Carbonates decompose at ~400 to 800°C depending on cation (*94*), suggesting that the carbonates on Bennu were not exposed to these higher temperatures, at least not for a sufficiently long period to decompose them all. The pervasive 2.7-μm hydration feature, with no spectral evidence for volumetrically abundant anhydrous silicates such as olivine and pyroxene (*3*), indicates that the phyllosilicate that is widespread on Bennu has not been dehydrated or decomposed (which is nearly complete by 700°C), nor has it formed detectable secondary olivine (which occurs by 800°C) (*95*).

The temperature and duration of aqueous alteration of the materials on Bennu, and their thermal metamorphism, will affect the abundance and distribution of both soluble and insoluble organic matter in the returned samples. The presence of aliphatic organics across Bennu's surface places a stricter limit on peak temperatures than the carbonates, because thermal alteration quickly destroys aliphatic bonds (*96*). The 3.4-μm spectral feature from aliphatic organics in insoluble organic matter (IOM) is lost within approximately 200 years at 100°C (*97*). CMs with organic spectral features therefore experienced <15°C heating over the duration of aqueous alteration, potentially further limiting the range of temperatures experienced by organic-rich regions on Bennu. It is possible that organic-rich boulders and carbonate-rich boulders are distinct populations (*40*, *41*), with different thermal histories. The thermal gradient within an asteroid parent body similar to Bennu's spans a range of hundreds of degrees Celsius (*73*), and this gradient, along with spatial heterogeneity in pore water flow, could account for the range of compositions inherited by Bennu.

Conclusions

Remote sensing observations provide outcrop-scale information, on scales larger than meteorite samples. Bennu shares compositional traits with aqueously altered CM and CI meteorites, including the presence of Mg-phyllosilicates, magnetite, and, we posit, carbonate mineralogy dominated by calcite, with smaller amounts of magnesite, dolomite, and breunnerite. However, the carbonate spectral dominance in OVIRS data at 3.4 μm is unusual compared to meteorite spectra. We observe bright veins with thicknesses of 3 to 15 cm and lengths that can exceed 1 m. We propose that they are composed of the spectrally detected carbonates. Based on the vein dimensions, which are much larger than any veins found in meteorites, a hydrothermal system of at least 89× the volume of the veins, or an amount of fluid at least 10^5× the volume of the veins, would have been required to leach the elements from the surrounding host rock. Fluid flow on Bennu's parent body would have taken place over distances of kilometers for thousands to millions of years. We predict that the returned sample could contain carbonates with distinct structure and scale from those in the meteorites.

It remains unclear whether these differences arise from material that would not survive delivery to Earth as a meteorite, or because Bennu's parent body is distinct from the CM or CI parent body. Bennu is unlikely to be unique in the asteroid population, as most asteroids have not been visited by spacecraft. Large-scale open-system hydrothermal alteration may therefore have occurred on carbonaceous parent bodies more generally. Ceres, the only other known carbonate-bearing asteroid that has been visited by a spacecraft, experienced extensive hydrothermal alteration, beyond the degree of the most hydrated (CI group) meteorites (*98*). This extensive alteration along with more recent geologic activity (*99*) may have obscured evidence of the earliest stages of alteration, including vein formation. Whether distinct or representative, the returned sample from Bennu is likely to contain carbon-bearing species in the form of organics and/or carbonates.

REFERENCES AND NOTES

1. D. S. Lauretta, S. S. Balram-Knutson, E. Beshore, W. V. Boynton, C. Drouet d'Aubigny, D. N. DellaGiustina, H. L. Enos, D. R. Golish, C. W. Hergenrother, E. S. Howell, C. A. Bennett, E. T. Morton, M. C. Nolan, B. Rizk, H. L. Roper, A. E. Bartels, B. J. Bos, J. P. Dworkin, D. E. Highsmith, D. A. Lorenz, L. F. Lim, R. Mink, M. C. Moreau, J. A. Nuth, D. C. Reuter, A. A. Simon, E. B. Bierhaus, B. H. Bryan, R. Ballouz, O. S. Barnouin, R. P. Binzel, W. F. Bottke, V. E. Hamilton, K. J. Walsh, S. R. Chesley, P. R. Christensen, B. E. Clark, H. C. Connolly, M. K. Crombie, M. G. Daly, J. P. Emery, T. J. McCoy, J. W. McMahon, D. J. Scheeres, S. Messenger, K. Nakamura-Messenger, K. Righter, S. A. Sandford, OSIRIS-REx: Sample Return from Asteroid (101955) Bennu. *Space Sci. Rev.* **212**, 925–984 (2017). doi:10.1007/s11214-017-0405-1
2. B. E. Clark, R. P. Binzel, E. S. Howell, E. A. Cloutis, M. Ockert-Bell, P. Christensen, M. A. Barucci, F. DeMeo, D. S. Lauretta, H. Connolly Jr., A. Soderberg, C. Hergenrother, L. Lim, J. Emery, M. Mueller, Asteroid (101955) 1999 RQ36: Spectroscopy from 0.4 to 2.4μm and meteorite analogs. *Icarus* **216**, 462–475 (2011). doi:10.1016/j.icarus.2011.08.021
3. V. E. Hamilton, A. A. Simon, P. R. Christensen, D. C. Reuter, B. E. Clark, M. A. Barucci, N. E. Bowles, W. V. Boynton, J. R. Brucato, E. A. Cloutis, H. C. Connolly Jr., K. L. D. Hanna, J. P. Emery, H. L. Enos, S. Fornasier, C. W. Haberle, R. D. Hanna, E. S. Howell, H. H. Kaplan, L. P. Keller, C. Lantz, J. Y. Li, L. F. Lim, T. J. McCoy, F. Merlin, M. C. Nolan, A. Praet, B. Rozitis, S. A. Sandford, D. L. Schrader, C. A. Thomas, X. D. Zou, D. S. Lauretta; OSIRIS-REx Team, Evidence for widespread hydrated minerals on asteroid (101955) Bennu. *Nat. Astron.* **3**, 332–340 (2019). doi:10.1038/s41550-019-0722-2 Medline
4. D. S. Lauretta, D. N. DellaGiustina, C. A. Bennett, D. R. Golish, K. J. Becker, S. S. Balram-Knutson, O. S. Barnouin, T. L. Becker, W. F. Bottke, W. V. Boynton, H. Campins, B. E. Clark, H. C. Connolly Jr., C. Y. Drouet d'Aubigny, J. P. Dworkin, J. P. Emery, H. L. Enos, V. E. Hamilton, C. W. Hergenrother, E. S. Howell, M. R. M. Izawa, H. H. Kaplan, M. C. Nolan, B. Rizk, H. L. Roper, D. J. Scheeres, P. H. Smith, K. J. Walsh, C. W. V. Wolner; OSIRIS-REx Team, The unexpected surface of asteroid (101955) Bennu. *Nature* **568**, 55–60 (2019). doi:10.1038/s41586-019-1033-6 Medline
5. D. DellaGiustina, J. Emery, D. Golish, B. Rozitis, C. Bennett, K. Burke, R.-L. Ballouz, K. Becker, P. Christensen, C. D. d'Aubigny, Properties of rubble-pile asteroid (101955) Bennu from OSIRIS-REx imaging and thermal analysis. *New Astron.* **3**, 341–351 (2019).
6. D. Takir, J. P. Emery, H. Y. Mcsween Jr., C. A. Hibbitts, R. N. Clark, N. Pearson, A. Wang, Nature and degree of aqueous alteration in CM and CI carbonaceous chondrites. *Meteorit. Planet. Sci.* **48**, 1618–1637 (2013). doi:10.1111/maps.12171
7. A. Ghosh, S. J. Weidenschilling, H. Y. McSween Jr., A. E. Rubin, in *Meteorites and the Early Solar System II* (Univ. of Arizona Press, 2006), pp. 555–566.
8. M. Endress, E. Zinner, A. Bischoff, Early aqueous activity on primitive meteorite parent bodies. *Nature* **379**, 701–703 (1996). doi:10.1038/379701a0 Medline
9. O. S. Barnouin, M. G. Daly, E. E. Palmer, R. W. Gaskell, J. R. Weirich, C. L. Johnson, M. M. A. Asad, J. H. Roberts, M. E. Perry, H. C. M. Susorney, R. T. Daly, E. B. Bierhaus, J. A. Seabrook, R. C. Espiritu, A. H. Nair, L. Nguyen, G. A. Neumann, C. M. Ernst, W. V. Boynton, M. C. Nolan, C. D. Adam, M. C. Moreau, B. Risk, C. D. D'Aubigny, E. R. Jawin, K. J. Walsh, P. Michel, S. R. Schwartz, R.-L. Ballouz, E. M. Mazarico, D. J. Scheeres, J. McMahon, W. Bottke, S. Sugita, N. Hirata, N. Hirata, S. Watanabe, K. N. Burke, D. N. DellaGuistina, C. A. Bennett, D. S. Lauretta; OSIRIS-REx Team., Shape of (101955) Bennu indicative of a rubble pile with internal stiffness. *Nat. Geosci.* **12**, 247–252 (2019). doi:10.1038/s41561-019-0330-x Medline
10. P. Michel, R.-L. Ballouz, O. S. Barnouin, M. Jutzi, K. J. Walsh, B. H. May, C. Manzoni, D. C. Richardson, S. R. Schwartz, S. Sugita, S. Watanabe, H. Miyamoto, M. Hirabayashi, W. F. Bottke, H. C. Connolly, M. Yoshikawa, D. S. Lauretta, Collisional formation of top-shaped asteroids and implications for the origins of Ryugu and Bennu. *Nat. Commun.* **11**, 2655 (2020). doi:10.1038/s41467-020-16433-z Medline
11. K. J. Walsh, M. Delbó, W. F. Bottke, D. Vokrouhlický, D. S. Lauretta, Introducing the Eulalia and new Polana asteroid families: Re-assessing primitive asteroid families in the inner Main Belt. *Icarus* **225**, 283–297 (2013). doi:10.1016/j.icarus.2013.03.005
12. W. R. Van Schmus, J. A. Wood, A chemical-petrologic classification for the chondritic meteorites. *Geochim. Cosmochim. Acta* **31**, 747–765 (1967). doi:10.1016/S0016-7037(67)80030-9
13. H. Y. McSween Jr., S. M. Richardson, The composition of carbonaceous chondrite matrix. *Geochim. Cosmochim. Acta* **41**, 1145–1161 (1977). doi:10.1016/0016-7037(77)90110-7
14. A. E. Rubin, J. M. Trigo-Rodríguez, H. Huber, J. T. Wasson, Progressive aqueous alteration of CM carbonaceous chondrites. *Geochim. Cosmochim. Acta* **71**, 2361–2382 (2007). doi:10.1016/j.gca.2007.02.008
15. M. E. Zolensky, D. W. Mittlefehldt, M. E. Lipschutz, M.-S. Wang, R. N. Clayton, T. K. Mayeda, M. M. Grady, C. Pillinger, D. B, D. B, CM chondrites exhibit the complete petrologic range from type 2 to 1. *Geochim. Cosmochim. Acta* **61**, 5099–5115 (1997). doi:10.1016/S0016-7037(97)00357-8
16. G. W. Kallemeyn, J. T. Wasson, The compositional classification of chondrites: IV. Ungrouped chondritic meteorites and clasts. *Geochim. Cosmochim. Acta* **49**, 261–270 (1985). doi:10.1016/0016-7037(85)90209-1
17. D. C. Reuter, A. A. Simon, J. Hair, A. Lunsford, S. Manthripragada, V. Bly, B. Bos, C. Brambora, E. Caldwell, G. Casto, Z. Dolch, P. Finneran, D. Jennings, M. Jhabvala, E. Matson, M. McLelland, W. Roher, T. Sullivan, E. Weigle, Y. Wen, D. Wilson, D. S.

Lauretta, The OSIRIS-REx Visible and InfraRed Spectrometer (OVIRS): Spectral Maps of the Asteroid Bennu. *Space Sci. Rev.* **214**, 54 (2018). doi:10.1007/s11214-018-0482-9
18. A. A. Simon, H. H. Kaplan, V. E. Hamilton, D. S. Lauretta, H. C. Campins, J. P. Emery, M. A. Barucci, D. N. DellaGiustina, D. C. Reuter, S. A. Sandford, D. R. Golish, L. F. Lim, A. Ryan, B. Rozitis, C. A. Bennett, Widespread carbon-bearing materials on near-Earth asteroid (101955) Bennu. *Science* 10.1126/science.abc3522 (2020). doi:10.1126/science.abc3522
19. Materials and methods are available as supplementary materials.
20. M. C. De Sanctis, E. Ammannito, H. Y. McSween, A. Raponi, S. Marchi, F. Capaccioni, M. T. Capria, F. G. Carrozzo, M. Ciarniello, S. Fonte, M. Formisano, A. Frigeri, M. Giardino, A. Longobardo, G. Magni, L. A. McFadden, E. Palomba, C. M. Pieters, F. Tosi, F. Zambon, C. A. Raymond, C. T. Russell, Localized aliphatic organic material on the surface of Ceres. *Science* **355**, 719–722 (2017). doi:10.1126/science.aaj2305 Medline
21. A. Raponi, M. Ciarniello, F. Capaccioni, V. Mennella, G. Filacchione, V. Vinogradoff, O. Poch, P. Beck, E. Quirico, M. C. De Sanctis, L. V. Moroz, D. Kappel, S. Erard, D. Bockelée-Morvan, A. Longobardo, F. Tosi, E. Palomba, J.-P. Combe, B. Rousseau, G. Arnold, R. W. Carlson, A. Pommerol, C. Pilorget, S. Fornasier, G. Bellucci, A. Barucci, F. Mancarella, M. Formisano, G. Rinaldi, I. Istiqomah, C. Leyrat, Infrared detection of aliphatic organics on a cometary nucleus. *New Astron.* **4**, 500–505 (2020).
22. A. S. Rivkin, J. P. Emery, Detection of ice and organics on an asteroidal surface. *Nature* **464**, 1322–1323 (2010). doi:10.1038/nature09028 Medline
23. H. H. Kaplan, R. E. Milliken, C. M. O. Alexander, C. D. K. Herd, Reflectance spectroscopy of insoluble organic matter (IOM) and carbonaceous meteorites. *Meteorit. Planet. Sci.* **54**, 1051–1068 (2019). doi:10.1111/maps.13264
24. M. Endress, A. Bischoff, Carbonates in CI chondrites: Clues to parent body evolution. *Geochim. Cosmochim. Acta* **60**, 489–507 (1996). doi:10.1016/0016-7037(95)00399-1 Medline
25. S. J. Gaffey, Spectral reflectance of carbonate minerals in the visible and near infrared (0.35–2.55 um): Anhydrous carbonate minerals. *J. Geophys. Res.* **92** (B2), 1429 (1987). doi:10.1029/JB092iB02p01429
26. M. C. De Sanctis, A. Raponi, E. Ammannito, M. Ciarniello, M. J. Toplis, H. Y. McSween, J. C. Castillo-Rogez, B. L. Ehlmann, F. G. Carrozzo, S. Marchi, F. Tosi, F. Zambon, F. Capaccioni, M. T. Capria, S. Fonte, M. Formisano, A. Frigeri, M. Giardino, A. Longobardo, G. Magni, E. Palomba, L. A. McFadden, C. M. Pieters, R. Jaumann, P. Schenk, R. Mugnuolo, C. A. Raymond, C. T. Russell, Bright carbonate deposits as evidence of aqueous alteration on (1) Ceres. *Nature* **536**, 54–57 (2016). doi:10.1038/nature18290 Medline
27. P. R. Christensen, V. E. Hamilton, G. L. Mehall, D. Pelham, W. O'Donnell, S. Anwar, H. Bowles, S. Chase, J. Fahlgren, Z. Farkas, T. Fisher, O. James, I. Kubik, I. Lazbin, M. Miner, M. Rassas, L. Schulze, K. Shamordola, T. Tourville, G. West, R. Woodward, D. Lauretta, The OSIRIS-REx Thermal Emission Spectrometer (OTES) Instrument. *Space Sci. Rev.* **214**, 87 (2018). doi:10.1007/s11214-018-0513-6
28. J. L. Bandfield, T. D. Glotch, P. R. Christensen, Spectroscopic identification of carbonate minerals in the martian dust. *Science* **301**, 1084–1087 (2003). doi:10.1126/science.1088054 Medline
29. K. C. Feely, P. R. Christensen, Quantitative compositional analysis using thermal emission spectroscopy: Application to igneous and metamorphic rocks. *J. Geophys. Res. Planets* **104** (E10), 24195–24210 (1999). doi:10.1029/1999JE001034
30. B. Rizk, C. Drouet d'Aubigny, D. Golish, C. Fellows, C. Merrill, P. Smith, M. S. Walker, J. E. Hendershot, J. Hancock, S. H. Bailey, D. N. DellaGiustina, D. S. Lauretta, R. Tanner, M. Williams, K. Harshman, M. Fitzgibbon, W. Verts, J. Chen, T. Connors, D. Hamara, A. Dowd, A. Lowman, M. Dubin, R. Burt, M. Whiteley, M. Watson, T. McMahon, M. Ward, D. Booher, M. Read, B. Williams, M. Hunten, E. Little, T. Saltzman, D. Alfred, S. O'Dougherty, M. Walthall, K. Kenagy, S. Peterson, B. Crowther, M. L. Perry, C. See, S. Selznick, C. Sauve, M. Beiser, W. Black, R. N. Pfisterer, A. Lancaster, S. Oliver, C. Oquest, D. Crowley, C. Morgan, C. Castle, R. Dominguez, M. Sullivan, OCAMS: The OSIRIS-REx Camera Suite. *Space Sci. Rev.* **214**, 26 (2018). doi:10.1007/s11214-017-0460-7
31. D. R. Golish, C. Drouet d'Aubigny, B. Rizk, D. N. DellaGiustina, P. H. Smith, K. Becker, N. Shultz, T. Stone, M. K. Barker, E. Mazarico, E. Tatsumi, R. W. Gaskell, L. Harrison, C. Merrill, C. Fellows, B. Williams, S. O'Dougherty, M. Whiteley, J. Hancock, B. E. Clark, C. W. Hergenrother, D. S. Lauretta, Ground and In-Flight Calibration of the OSIRIS-REx Camera Suite. *Space Sci. Rev.* **216**, 12 (2020). doi:10.1007/s11214-019-0626-6 Medline
32. O. S. Barnouin, M. G. Daly, E. E. Palmer, C. L. Johnson, R. W. Gaskell, M. Al Asad, E. B. Bierhaus, K. L. Craft, C. M. Ernst, R. C. Espiritu, H. Nair, G. A. Neumann, L. Nguyen, M. C. Nolan, E. Mazarico, M. E. Perry, L. C. Philpott, J. H. Roberts, R. J. Steele, J. Seabrook, H. C. M. Susorney, J. R. Weirich, D. S. Lauretta, Digital terrain mapping by the OSIRIS-REx mission. *Planet. Space Sci.* **180**, 104764 (2020). doi:10.1016/j.pss.2019.104764
33. D. R. Golish, D. N. DellaGiustina, J.-Y. Li, B. E. Clark, X.-D. Zou, P. H. Smith, J. L. Rizos, P. H. Hasselmann, C. A. Bennett, S. Fornasier, R.-L. Ballouz, C. Drouet d'Aubigny, B. Rizk, M. G. Daly, O. S. Barnouin, L. Philpott, M. M. Al Asad, J. A. Seabrook, C. L. Johnson, D. S. Lauretta, Disk-resolved photometric modeling and properties of asteroid (101955) Bennu. *Icarus* 10.1016/j.icarus.2020.113724 (2020). doi:10.1016/j.icarus.2020.113724
34. C. W. Hergenrother, C. K. Maleszewski, M. C. Nolan, J.-Y. Li, C. Y. Drouet d'Aubigny, F. C. Shelly, E. S. Howell, T. R. Kareta, M. R. M. Izawa, M. A. Barucci, E. B. Bierhaus, H. Campins, S. R. Chesley, B. E. Clark, E. J. Christensen, D. N. DellaGiustina, S. Fornasier, D. R. Golish, C. M. Hartzell, B. Rizk, D. J. Scheeres, P. H. Smith, X.-D. Zou, D. S. Lauretta; OSIRIS-REx Team, The operational environment and rotational acceleration of asteroid (101955) Bennu from OSIRIS-REx observations. *Nat. Commun.* **10**, 1291 (2019). doi:10.1038/s41467-019-09213-x Medline
35. T. G. Sharp, P. S. DeCarli, in *Meteorites and the Early Solar System II* (Univ. of Arizona Press, 2006), pp. 653–677.
36. S. Sugita, R. Honda, T. Morota, S. Kameda, H. Sawada, E. Tatsumi, M. Yamada, C. Honda, Y. Yokota, T. Kouyama, N. Sakatani, K. Ogawa, H. Suzuki, T. Okada, N. Namiki, S. Tanaka, Y. Iijima, K. Yoshioka, M. Hayakawa, Y. Cho, M. Matsuoka, N. Hirata, N. Hirata, H. Miyamoto, D. Domingue, M. Hirabayashi, T. Nakamura, T. Hiroi, T. Michikami, P. Michel, R.-L. Ballouz, O. S. Barnouin, C. M. Ernst, S. E. Schröder, H. Kikuchi, R. Hemmi, G. Komatsu, T. Fukuhara, M. Taguchi, T. Arai, H. Senshu, H. Demura, Y. Ogawa, Y. Shimaki, T. Sekiguchi, T. G. Müller, A. Hagermann, T. Mizuno, H. Noda, K. Matsumoto, R. Yamada, Y. Ishihara, H. Ikeda, H. Araki, K. Yamamoto, S. Abe, F. Yoshida, A. Higuchi, S. Sasaki, S. Oshigami, S. Tsuruta, K. Asari, S. Tazawa, M. Shizugami, J. Kimura, T. Otsubo, H. Yabuta, S. Hasegawa, M. Ishiguro, S. Tachibana, E. Palmer, R. Gaskell, L. Le Corre, R. Jaumann, K. Otto, N. Schmitz, P. A. Abell, M. A. Barucci, M. E. Zolensky, F. Vilas, F. Thuillet, C. Sugimoto, N. Takaki, Y. Suzuki, H. Kamiyoshihara, M. Okada, K. Nagata, M. Fujimoto, M. Yoshikawa, Y. Yamamoto, K. Shirai, R. Noguchi, N. Ogawa, F. Terui, S. Kikuchi, T. Yamaguchi, Y. Oki, Y. Takao, H. Takeuchi, G. Ono, Y. Mimasu, K. Yoshikawa, T. Takahashi, Y. Takei, A. Fujii, C. Hirose, S. Nakazawa, S. Hosoda, O. Mori, T. Shimada, S. Soldini, T. Iwata, M. Abe, H. Yano, R. Tsukizaki, M. Ozaki, K. Nishiyama, T. Saiki, S. Watanabe, Y. Tsuda, The geomorphology, color, and thermal properties of Ryugu: Implications for parent-body processes. *Science* **364**, 252 (2019). doi:10.1126/science.aaw0422 Medline
37. D. N. DellaGiustina *et al*., Variation in color and reflectance of asteroid (101955) Bennu. *Science* (2020). 10.1126/science.abc3660
38. B. Rozitis *et al*., Asteroid (101955) Bennu's Weak Boulders and Thermally Anomalous Equator. *Sci. Adv.* (2020). 10.1126/sciadv.abc3699
39. M. R. Lee, P. Lindgren, M. R. Sofe, Aragonite, breunnerite, calcite and dolomite in the CM carbonaceous chondrites: High fidelity recorders of progressive parent body aqueous alteration. *Geochim. Cosmochim. Acta* **144**, 126–156 (2014). doi:10.1016/j.gca.2014.08.019
40. K. T. Howard, C. M. O. Alexander, D. L. Schrader, K. A. Dyl, Classification of hydrous meteorites (CR, CM and C2 ungrouped) by phyllosilicate fraction: PSD-XRD modal mineralogy and planetesimal environments. *Geochim. Cosmochim. Acta* **149**, 206–222 (2015). doi:10.1016/j.gca.2014.10.025
41. C. M. O. Alexander, R. Bowden, M. L. Fogel, K. T. Howard, Carbonate abundances and isotopic compositions in chondrites. *Meteorit. Planet. Sci.* **50**, 810–833 (2015). doi:10.1111/maps.12410
42. M. R. Lee, P. Lindgren, M. R. Sofe, C. M. O'D Alexander, J. Wang, C. M. O'D Alexander, J. Wang, Extended chronologies of aqueous alteration in the CM2 carbonaceous chondrites: Evidence from carbonates in Queen Alexandra Range 93005. *Geochim. Cosmochim. Acta* **92**, 148–169 (2012). doi:10.1016/j.gca.2012.06.005

43. S. De Leuw, A. E. Rubin, J. T. Wasson, Carbonates in CM chondrites: Complex formational histories and comparison to carbonates in CI chondrites. *Meteorit. Planet. Sci.* **45**, 513–530 (2010). doi:10.1111/j.1945-5100.2010.01037.x
44. L. R. Riciputi, H. Y. McSween Jr., C. A. Johnson, M. Prinz, Minor and trace element concentrations in carbonates of carbonaceous chondrites, and implications for the compositions of coexisting fluids. *Geochim. Cosmochim. Acta* **58**, 1343–1351 (1994). doi:10.1016/0016-7037(94)90386-7
45. J. Alfing, M. Patzek, A. Bischoff, Modal abundances of coarse-grained (>5 µm) components within CI-chondrites and their individual clasts – Mixing of various lithologies on the CI parent body(ies). *Geochemistry* **79**, 125532 (2019). doi:10.1016/j.chemer.2019.08.004
46. K. Fredriksson, J. F. Kerridge, Carbonates and sulfates in CI chondrites: Formation by aqueous activity on the parent body. *Meteoritics* **23**, 35–44 (1988). doi:10.1111/j.1945-5100.1988.tb00894.x Medline
47. C. A. Johnson, M. Prinz, Carbonate compositions in CM and CI chondrites and implications for aqueous alteration. *Geochim. Cosmochim. Acta* **57**, 2843–2852 (1993). doi:10.1016/0016-7037(93)90393-B
48. T. Nakamura, Yamato 793321 CM chondrite: Dehydrated regolith material of a hydrous asteroid. *Earth Planet. Sci. Lett.* **242**, 26–38 (2006). doi:10.1016/j.epsl.2005.11.040
49. M. K. Weisberg, M. Prinz, R. N. Clayton, T. K. Mayeda, The CR (Renazzo-type) carbonaceous chondrite group and its implications. *Geochim. Cosmochim. Acta* **57**, 1567–1586 (1993). doi:10.1016/0016-7037(93)90013-M
50. M. R. Lee, M. R. Sofe, P. Lindgren, N. A. Starkey, I. A. Franchi, The oxygen isotope evolution of parent body aqueous solutions as recorded by multiple carbonate generations in the Lonewolf Nunataks 94101 CM2 carbonaceous chondrite. *Geochim. Cosmochim. Acta* **121**, 452–466 (2013). doi:10.1016/j.gca.2013.07.010
51. S. M. Richardson, Vein formation in the C1 carbonaceous chondrites. *Meteoritics* **13**, 141–159 (1978). doi:10.1111/j.1945-5100.1978.tb00803.x
52. K. Tomeoka, in *Proceedings of the NIPR Symposum*, K. Yanai, Ed. (National Institute of Polar Research, 1990), vol. 3.
53. C. E. Jilly-Rehak, G. R. Huss, K. Nagashima, 53 Mn– 53 Cr radiometric dating of secondary carbonates in CR chondrites: Timescales for parent body aqueous alteration. *Geochim. Cosmochim. Acta* **201**, 224–244 (2017). doi:10.1016/j.gca.2016.08.033
54. K. Tomeoka, Phyllosilicate veins in a CI meteorite: Evidence for aqueous alteration on the parent body. *Nature* **345**, 138–140 (1990). doi:10.1038/345138a0
55. M. R. Lee, K. Nicholson, Ca-carbonate in the Orgueil (CI) carbonaceous chondrite: Mineralogy, microstructure and implications for parent body history. *Earth Planet. Sci. Lett.* **280**, 268–275 (2009). doi:10.1016/j.epsl.2009.01.038
56. N. P. Hanowski, A. J. Brearley, Iron-rich aureoles in the CM carbonaceous chondrites Murray, Murchison, and Allan Hills 81002: Evidence for *in situ* aqueous alteration. *Meteorit. Planet. Sci.* **35**, 1291–1308 (2000). doi:10.1111/j.1945-5100.2000.tb01517.x
57. M. Gounelle, M. E. Zolensky, A terrestrial origin for sulfate veins in CI1 chondrites. *Meteorit. Planet. Sci.* **36**, 1321–1329 (2001). doi:10.1111/j.1945-5100.2001.tb01827.x
58. P. Lindgren, M. R. Lee, M. Sofe, M. J. Burchell, Microstructure of calcite in the CM2 carbonaceous chondrite LON 94101: Implications for deformation history during and/or after aqueous alteration. *Earth Planet. Sci. Lett.* **306**, 289–298 (2011). doi:10.1016/j.epsl.2011.04.022
59. D. N. DellaGiustina, H. H. Kaplan, A. A. Simon, W. F. Bottke, C. Avdellidou, M. Delbo, R.-L. Ballouz, D. R. Golish, K. J. Walsh, M. Popescu, H. Campins, M. A. Barucci, G. Poggiali, R. T. Daly, L. Le Corre, V. E. Hamilton, N. Porter, E. R. Jawin, T. J. McCoy, H. C. Connolly Jr., J. L. R. Garcia, E. Tatsumi, J. de Leon, J. Licandro, S. Fornasier, M. G. Daly, M. M. Al Asad, L. Philpott, J. Seabrook, O. S. Barnouin, B. E. Clark, M. C. Nolan, E. S. Howell, R. P. Binzel, B. Rizk, D. C. Reuter, D. S. Lauretta, Exogenic Basalt on Asteroid (101955) Bennu. *New Astron.* 10.1038/s41550-020-1195-z (2020). doi:10.1038/s41550-020-1195-z
60. E. A. Cloutis, T. Hiroi, M. J. Gaffey, C. M. O. Alexander, P. Mann, Spectral reflectance properties of carbonaceous chondrites: 1. CI chondrites. *Icarus* **212**, 180–209 (2011). doi:10.1016/j.icarus.2010.12.009
61. M. R. M. Izawa, E. A. Cloutis, T. Rhind, S. A. Mertzman, D. M. Applin, J. M. Stromberg, D. M. Sherman, Spectral reflectance properties of magnetites: Implications for remote sensing. *Icarus* **319**, 525–539 (2019). doi:10.1016/j.icarus.2018.10.002
62. E. A. Cloutis, S. E. Grasby, W. M. Last, R. Léveillé, G. R. Osinski, B. L. Sherriff, Spectral reflectance properties of carbonates from terrestrial analogue environments: Implications for Mars. *Planet. Space Sci.* **58**, 522–537 (2010). doi:10.1016/j.pss.2009.09.002
63. R. N. Clark, Spectral properties of mixtures of montmorillonite and dark carbon grains: Implications for remote sensing minerals containing chemically and physically adsorbed water. *J. Geophys. Res.* **88**, 10635–10644 (1983). doi:10.1029/JB088iB12p10635
64. A. Le Bras, S. Erard, Reflectance spectra of regolith analogs in the mid-infrared: Effects of grain size. *Planet. Space Sci.* **51**, 281–294 (2003). doi:10.1016/S0032-0633(03)00017-5
65. R. J. P. Lyon, W. M. Tuddenham, C. S. Thompson, Quantitative mineralogy in 30 minutes. *Econ. Geol.* **54**, 1047–1055 (1959). doi:10.2113/gsecongeo.54.6.1047
66. A. D. Rogers, O. Aharonson, Mineralogical composition of sands in Meridiani Planum determined from Mars Exploration Rover data and comparison to orbital measurements. *J. Geophys. Res.* **113**, E06S14 (2008). doi:10.1029/2007JE002995
67. R. E. Grimm, H. Y. Mcsween Jr., Water and the thermal evolution of carbonaceous chondrite parent bodies. *Icarus* **82**, 244–280 (1989). doi:10.1016/0019-1035(89)90038-9
68. A. J. Brearley, M. Prinz, CI chondrite-like clasts in the Nilpena polymict ureilite: Implications for aqueous alteration processes in CI chondrites. *Geochim. Cosmochim. Acta* **56**, 1373–1386 (1992). doi:10.1016/0016-7037(92)90068-T
69. M. Zolensky, R. Barrett, L. Browning, Mineralogy and composition of matrix and chondrule rims in carbonaceous chondrites. *Geochim. Cosmochim. Acta* **57**, 3123–3148 (1993). doi:10.1016/0016-7037(93)90298-B
70. E. R. Dufresne, E. Anders, On the chemical evolution of the carbonaceous chondrites. *Geochim. Cosmochim. Acta* **26**, 1085–1114 (1962). doi:10.1016/0016-7037(62)90047-9
71. R. N. Clayton, T. K. Mayeda, Oxygen isotope studies of carbonaceous chondrites. *Geochim. Cosmochim. Acta* **63**, 2089–2104 (1999). doi:10.1016/S0016-7037(99)00090-3
72. P. A. Bland, M. D. Jackson, R. F. Coker, B. A. Cohen, J. B. W. Webber, M. R. Lee, C. M. Duffy, R. J. Chater, M. G. Ardakani, D. S. McPhail, D. W. McComb, G. K. Benedix, Why aqueous alteration in asteroids was isochemical: High porosity≠high permeability. *Earth Planet. Sci. Lett.* **287**, 559–568 (2009). doi:10.1016/j.epsl.2009.09.004
73. E. D. Young, R. D. Ash, P. England, D. Rumble 3rd, Fluid flow in chondritic parent bodies: Deciphering the compositions of planetesimals. *Science* **286**, 1331–1335 (1999). doi:10.1126/science.286.5443.1331 Medline
74. E. D. Young, The hydrology of carbonaceous chondrite parent bodies and the evolution of planet progenitors. *Philos. Trans.- Royal Soc., Math. Phys. Eng. Sci.* **359**, 2095–2110 (2001). doi:10.1098/rsta.2001.0900
75. B. Travis, G. Schubert, Hydrothermal convection in carbonaceous chondrite parent bodies. *Earth Planet. Sci. Lett.* **240**, 234–250 (2005). doi:10.1016/j.epsl.2005.09.008
76. E. D. Young, K. K. Zhang, G. Schubert, Conditions for pore water convection within carbonaceous chondrite parent bodies – implications for planetesimal size and heat production. *Earth Planet. Sci. Lett.* **213**, 249–259 (2003). doi:10.1016/S0012-821X(03)00345-5
77. J. Palguta, G. Schubert, B. J. Travis, Fluid flow and chemical alteration in carbonaceous chondrite parent bodies. *Earth Planet. Sci. Lett.* **296**, 235–243 (2010). doi:10.1016/j.epsl.2010.05.003
78. P. A. Bland, B. J. Travis, Giant convecting mud balls of the early solar system. *Sci. Adv.* **3**, e1602514 (2017). doi:10.1126/sciadv.1602514 Medline
79. Y.-J. Lee, J. W. Morse, Calcite precipitation in synthetic veins: Implications for the time and fluid volume necessary for vein filling. *Chem. Geol.* **156**, 151–170 (1999). doi:10.1016/S0009-2541(98)00183-1
80. M. A. Tyra, J. Farquhar, Y. Guan, L. A. Leshin, An oxygen isotope dichotomy in CM2 chondritic carbonates—A SIMS approach. *Geochim. Cosmochim. Acta* **77**, 383–395 (2012). doi:10.1016/j.gca.2011.10.003
81. L. Wilson, K. Keil, S. J. Love, The internal structures and densities of asteroids. *Meteorit. Planet. Sci.* **34**, 479–483 (1999). doi:10.1111/j.1945-5100.1999.tb01355.x

82. P. Hoppe, D. MacDougall, G. W. Lugmair, High spatial resolution ion microprobe measurements refine chronology of carbonate formation in Orgueil. *Meteorit. Planet. Sci.* **42**, 1309–1320 (2007). doi:10.1111/j.1945-5100.2007.tb00576.x
83. M. Telus, C. M. O. Alexander, E. H. Hauri, J. Wang, Calcite and dolomite formation in the CM parent body: Insight from in situ C and O isotope analyses. *Geochim. Cosmochim. Acta* **260**, 275–291 (2019). doi:10.1016/j.gca.2019.06.012
84. W. Fujiya, N. Sugiura, H. Hotta, K. Ichimura, Y. Sano, Evidence for the late formation of hydrous asteroids from young meteoritic carbonates. *Nat. Commun.* **3**, 627 (2012). doi:10.1038/ncomms1635 Medline
85. C. E. Jilly, G. R. Huss, A. N. Krot, K. Nagashima, Q.-Z. Yin, N. Sugiura, ^{53}Mn-^{53}Cr dating of aqueously formed carbonates in the CM2 lithology of the Sutter's Mill carbonaceous chondrite. *Meteorit. Planet. Sci.* **49**, 2104–2117 (2014). doi:10.1111/maps.12305
86. E. Tonui, M. Zolensky, T. Hiroi, T. Nakamura, M. E. Lipschutz, M.-S. Wang, K. Okudaira, Petrographic, chemical and spectroscopic evidence for thermal metamorphism in carbonaceous chondrites I: CI and CM chondrites. *Geochim. Cosmochim. Acta* **126**, 284–306 (2014). doi:10.1016/j.gca.2013.10.053
87. M. E. Zolensky, N. M. Abreu, M. A. Velbel, A. Rubin, N. Chaumard, T. Noguchi, T. Michikami, in *Primitive Meteorites and Asteroids* (Elsevier, 2018; https://linkinghub.elsevier.com/retrieve/pii/B9780128133255000021), pp. 59–204.
88. T. Nakamura, T. Noguchi, M. E. Zolensky, M. Tanaka, Mineralogy and noble-gas signatures of the carbonate-rich lithology of the Tagish Lake carbonaceous chondrite: Evidence for an accretionary breccia. *Earth Planet. Sci. Lett.* **207**, 83–101 (2003). doi:10.1016/S0012-821X(02)01127-5
89. P. G. Brown, A. R. Hildebrand, M. E. Zolensky, M. Grady, R. N. Clayton, T. K. Mayeda, E. Tagliaferri, R. Spalding, N. D. MacRae, E. L. Hoffman, D. W. Mittlefehldt, J. F. Wacker, J. A. Bird, M. D. Campbell, R. Carpenter, H. Gingerich, M. Glatiotis, E. Greiner, M. J. Mazur, P. J. McCausland, H. Plotkin, T. Rubak Mazur, The fall, recovery, orbit, and composition of the Tagish Lake meteorite: A new type of carbonaceous chondrite. *Science* **290**, 320–325 (2000). doi:10.1126/science.290.5490.320 Medline
90. C. Lantz, R. Brunetto, M. A. Barucci, S. Fornasier, D. Baklouti, J. Bourçois, M. Godard, Ion irradiation of carbonaceous chondrites: A new view of space weathering on primitive asteroids. *Icarus* **285**, 43–57 (2017). doi:10.1016/j.icarus.2016.12.019
91. M. S. Thompson, M. J. Loeffler, R. V. Morris, L. P. Keller, R. Christoffersen, Spectral and chemical effects of simulated space weathering of the Murchison CM2 carbonaceous chondrite. *Icarus* **319**, 499–511 (2019). doi:10.1016/j.icarus.2018.09.022
92. D. S. Lauretta, C. W. Hergenrother, S. R. Chesley, J. M. Leonard, J. Y. Pelgrift, C. D. Adam, M. Al Asad, P. G. Antreasian, R.-L. Ballouz, K. J. Becker, C. A. Bennett, B. J. Bos, W. F. Bottke, M. Brozović, H. Campins, H. C. Connolly Jr., M. G. Daly, A. B. Davis, J. de León, D. N. DellaGiustina, C. Y. Drouet d'Aubigny, J. P. Dworkin, J. P. Emery, D. Farnocchia, D. P. Glavin, D. R. Golish, C. M. Hartzell, R. A. Jacobson, E. R. Jawin, P. Jenniskens, J. N. Kidd Jr., E. J. Lessac-Chenen, J.-Y. Li, G. Libourel, J. Licandro, A. J. Liounis, C. K. Maleszewski, C. Manzoni, B. May, L. K. McCarthy, J. W. McMahon, P. Michel, J. L. Molaro, M. C. Moreau, D. S. Nelson, W. M. Owen Jr., B. Rizk, H. L. Roper, B. Rozitis, E. M. Sahr, D. J. Scheeres, J. A. Seabrook, S. H. Selznick, Y. Takahashi, F. Thuillet, P. Tricarico, D. Vokrouhlický, C. W. V. Wolner, Episodes of particle ejection from the surface of the active asteroid (101955) Bennu. *Science* **366**, eaay3544 (2019). doi:10.1126/science.aay3544 Medline
93. E. B. Bierhaus, B. C. Clark, J. W. Harris, K. S. Payne, R. D. Dubisher, D. W. Wurts, R. A. Hund, R. M. Kuhns, T. M. Linn, J. L. Wood, A. J. May, J. P. Dworkin, E. Beshore, D. S. Lauretta, The OSIRIS-REx Spacecraft and the Touch-and-Go Sample Acquisition Mechanism (TAGSAM). *Space Sci. Rev.* **214**, 107 (2018). doi:10.1007/s11214-018-0521-6
94. E. K. Tonui, M. E. Zolensky, M. E. Lipschutz, M.-S. Wang, T. Nakamura, Yamato 86029: Aqueously altered and thermally metamorphosed CI-like chondrite with unusual textures. *Meteorit. Planet. Sci.* **38**, 269–292 (2003). doi:10.1111/j.1945-5100.2003.tb00264.x
95. W. Nozaki, T. Nakamura, T. Noguchi, Bulk mineralogical changes of hydrous micrometeorites during heating in the upper atmosphere at temperatures below 1000 °C. *Meteorit. Planet. Sci.* **41**, 1095–1114 (2006). doi:10.1111/j.1945-5100.2006.tb00507.x
96. C. M. O. Alexander, G. D. Cody, B. T. De Gregorio, L. R. Nittler, R. M. Stroud, The nature, origin and modification of insoluble organic matter in chondrites, the major source of Earth's C and N. *Chem. Erde Geochem.* **77**, 227–256 (2017). doi:10.1016/j.chemer.2017.01.007 Medline
97. Y. Kebukawa, S. Nakashima, M. E. Zolensky, Kinetics of organic matter degradation in the Murchison meteorite for the evaluation of parent-body temperature history. *Meteorit. Planet. Sci.* **45**, 99–113 (2010). doi:10.1111/j.1945-5100.2009.01008.x
98. H. Y. McSween Jr., J. P. Emery, A. S. Rivkin, M. J. Toplis, J. C. Castillo-Rogez, T. H. Prettyman, M. C. De Sanctis, C. M. Pieters, C. A. Raymond, C. T. Russell, Carbonaceous chondrites as analogs for the composition and alteration of Ceres. *Meteorit. Planet. Sci.* **53**, 1793–1804 (2017). doi:10.1111/maps.12947
99. H. Hiesinger, S. Marchi, N. Schmedemann, P. Schenk, J. H. Pasckert, A. Neesemann, D. P. O'Brien, T. Kneissl, A. I. Ermakov, R. R. Fu, M. T. Bland, A. Nathues, T. Platz, D. A. Williams, R. Jaumann, J. C. Castillo-Rogez, O. Ruesch, B. Schmidt, R. S. Park, F. Preusker, D. L. Buczkowski, C. T. Russell, C. A. Raymond, Cratering on Ceres: Implications for its crust and evolution. *Science* **353**, aaf4759 (2016). doi:10.1126/science.aaf4759 Medline
100. A. Simon, D. Reuter, N. Gorius, A. Lunsford, R. Cosentino, G. Wind, D. Lauretta, the OSIRIS-REx Team, In-Flight Calibration and Performance of the OSIRIS-REx Visible and IR Spectrometer (OVIRS). *Remote Sens.* **10**, 1486 (2018). doi:10.3390/rs10091486
101. Reflectance Experiment Laboratory (RELAB) Spectral Database, (2020), http://www.planetary.brown.edu/relab/
102. R. F. Kokaly, R. N. Clark, G. A. Swayze, K. E. Livo, T. M. Hoefen, N. C. Pearson, R. A. Wise, W. M. Benzel, H. A. Lowers, R. L. Driscoll, A. J. Klein, "USGS Spectral Library Version 7," *Data Series* (Report 1035, Reston, VA, 2017), p. 68.
103. F. A. Kruse, A. B. Lefkoff, J. B. Dietz, Expert system-based mineral mapping in northern death valley, California/Nevada, using the Airborne Visible/Infrared Imaging Spectrometer (AVIRIS). *Remote Sens. Environ.* **44**, 309–336 (1993). doi:10.1016/0034-4257(93)90024-R
104. R. B. Singer, T. B. McCord, Mars - Large scale mixing of bright and dark surface materials and implications for analysis of spectral reflectance, in *Lunar and Planetary Science Conference, 10th, Houston, Tex. March 19-23, 1979, Proceedings* (Pergamon, 1979), vol. 2, pp. 1835–1848.
105. B. Hapke, Bidirectional reflectance spectroscopy: 1. Theory. *J. Geophys. Res. Solid Earth* **86** (B4), 3039–3054 (1981). doi:10.1029/JB086iB04p03039
106. D. N. DellaGiustina, C. A. Bennett, K. Becker, D. R. Golish, L. Le Corre, D. A. Cook, K. L. Edmundson, M. Chojnacki, S. S. Sutton, M. P. Milazzo, B. Carcich, M. C. Nolan, N. Habib, K. N. Burke, T. Becker, P. H. Smith, K. J. Walsh, K. Getzandanner, D. R. Wibben, J. M. Leonard, M. M. Westermann, A. T. Polit, J. N. Kidd Jr., C. W. Hergenrother, W. V. Boynton, J. Backer, S. Sides, J. Mapel, K. Berry, H. Roper, C. Drouet d'Aubigny, B. Rizk, M. K. Crombie, E. K. Kinney-Spano, J. de León, J. L. Rizos, J. Licandro, H. C. Campins, B. E. Clark, H. L. Enos, D. S. Lauretta, Overcoming the Challenges Associated with Image-Based Mapping of Small Bodies in Preparation for the OSIRIS-REx Mission to (101955) Bennu. *Earth Space Sci.* **5**, 929–949 (2018). doi:10.1029/2018EA000382
107. M. G. Daly, O. S. Barnouin, C. Dickinson, J. Seabrook, C. L. Johnson, G. Cunningham, T. Haltigin, D. Gaudreau, C. Brunet, I. Aslam, A. Taylor, E. B. Bierhaus, W. Boynton, M. Nolan, D. S. Lauretta, The OSIRIS-REx Laser Altimeter (OLA) Investigation and Instrument. *Space Sci. Rev.* **212**, 899–924 (2017). doi:10.1007/s11214-017-0375-3
108. M. G. Daly, O. S. Barnouin, J. A. Seabrook, J. Roberts, C. Dickinson, K. J. Walsh, E. R. Jawin, E. E. Palmer, R. Gaskell, J. Weirich, T. Haltigin, D. Gaudreau, C. Brunet, G. Cunningham, P. Michel, Y. Zhang, R.-L. Ballouz, G. Neumann, M. E. Perry, L. Philpott, M. M. Al-Asad, C. L. Johnson, C. D. Adam, J. M. Leonard, J. L. Geeraert, K. Getzandanner, M. C. Nolan, R. T. Daly, E. B. Bierhaus, E. Mazarico, B. Rozitis, A. J. Ryan, D. Dellaguistina, B. Rizk, H. C. M. Susorney, H. L. Enos, D. S. Lauretta, Hemispherical Differences in the Shape and Topography of Asteroid (101955) Bennu. *Sci. Adv.* (2020). 10.1126/sciadv.abd3649
109. M. Kazhdan, H. Hoppe, Screened poisson surface reconstruction. *ACM Trans. Graph.* **32**, 1–13 (2013). doi:10.1145/2487228.2487237
110. Y.-J. Lee, J. W. Morse, D. V. Wiltschko, An experimentally verified model for calcite precipitation in veins. *Chem. Geol.* **130**, 203–215 (1996). doi:10.1016/0009-2541(96)00008-3

111. W. F. Bottke, D. Vokrouhlický, K. J. Walsh, M. Delbo, P. Michel, D. S. Lauretta, H. Campins, H. C. Connolly, D. J. Scheeres, S. R. Chelsey, In search of the source of asteroid (101955) Bennu: Applications of the stochastic YORP model. *Icarus* **247**, 191–217 (2015). doi:10.1016/j.icarus.2014.09.046
112. K. L. Donaldson Hanna, D. L. Schrader, E. A. Cloutis, G. D. Cody, A. J. King, T. J. McCoy, D. M. Applin, J. P. Mann, N. E. Bowles, J. R. Brucato, H. C. Connolly Jr., E. Dotto, L. P. Keller, L. F. Lim, B. E. Clark, V. E. Hamilton, C. Lantz, D. S. Lauretta, S. S. Russell, P. F. Schofield, Spectral characterization of analog samples in anticipation of OSIRIS-REx's arrival at Bennu: A blind test study. *Icarus* **319**, 701–723 (2019). doi:10.1016/j.icarus.2018.10.018

ACKNOWLEDGMENTS

We are grateful to C.W.V. Wolner for editorial review. We acknowledge the entire OSIRIS-REx Team for making the encounter with Bennu possible. **Funding:** Supported by NASA under Contract NNM10AA11C issued through the New Frontiers Program. **Author contributions:** H.H.K., D.S.L., A.A.S., and V.E.H. contributed to the conceptualization, formal analysis, and methodology of the paper; H.H.K., A.A.S., V.E.H., C.A.B., D.N.D., D.R.G., D.C.R., J.P.E., K.N.B., X.-D.Z., M.G.D., O.S.B., and J.A.S. performed data curation; H.H.K. was primarily responsible for visualization; K.I., N.P. and E.R.J. contributed methodology and formal analysis and helped with visualization; T.D.G. carried out investigation; D.S.L. and H.L.E. are responsible for project administration; H.H.K., D.S.L., A.A.S. V.E.H., D.N.D., D.R.G., D.C.R., K.N.B., H.C., H.C.C., J.P.D., J.P.E., D.P.G., T.D.G., R.H., K.I., E.R.J., T.J.M., N.P., S.A.S., S.F., B.E.C., X.-D.Z., M.G.D., O.S.B., and J.A.S. contributed to writing the original draft of this paper and contribution of ideas. **Competing interests:** We declare no competing interests. **Data and materials availability:** OVIRS spectral data from the Reconnaissance A phase are available via the Planetary Data System (PDS) at https://sbn.psi.edu/pds/resource/orex/ovirs.html; data from the Nightingale site flyby have filenames starting with the dates of data collection, 2019-10-26 to 2019-10-27 . OCAMS (PolyCam) images from the Reconnaissance A phase are available on the PDS at https://sbn.psi.edu/pds/resource/orex/ocams.html. File names for the data we used are given in Table S3. Calcite, siderite, magnesite, and dolomite laboratory spectra (Figs. 1, 2 and 3) were taken from RELAB (http://www.planetary.brown.edu/relab/) and the USGS Spectral Library (https://www.sciencebase.gov/catalog/item/5807a2a2e4b0841e59e3a18d); the spectra identifiers we used are listed in table S1. A catalog of our spectral classifications is provided in Data S1.

SUPPLEMENTARY MATERIALS

science.sciencemag.org/cgi/content/full/science.abc3557/DC1
Materials and Methods
Figs. S1 to S11
Tables S1 to S4
References (*100–112*)
Data S1

20 April 2020; accepted 24 September 2020
Published online 8 October 2020
10.1126/science.abc3557

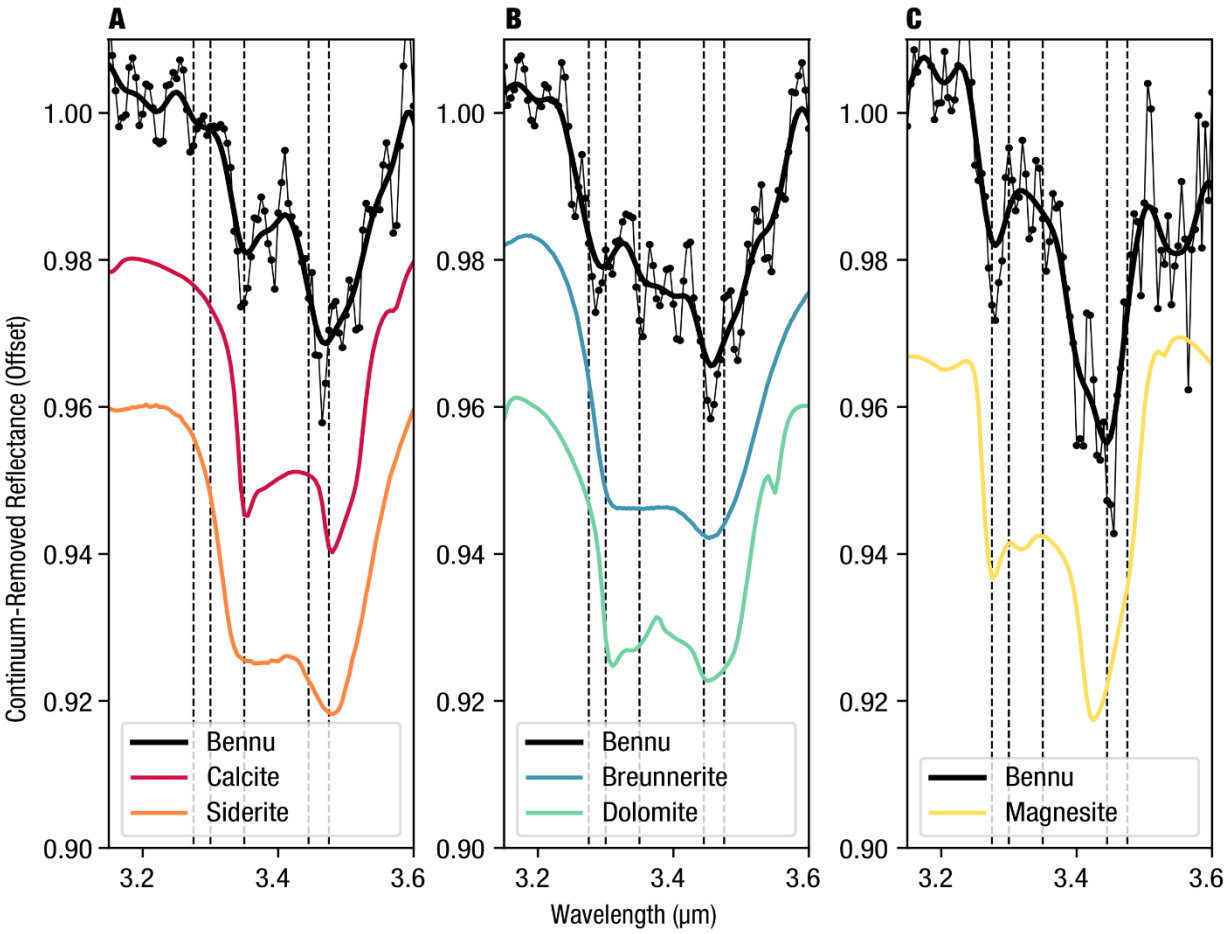

Fig. 1. Spectral features in OVIRS data compared to laboratory carbonate spectra. (**A** to **C**) Black points show the original OVIRS spectrum of Bennu from three different locations in Nightingale, and the thick black lines are the spectrum smoothed with a 3σ Gaussian. The carbonate laboratory spectra (colored lines as indicated in the legends) are natural, terrestrial samples with variable cation content (table S1). All spectra have had their continuum removed and are offset.

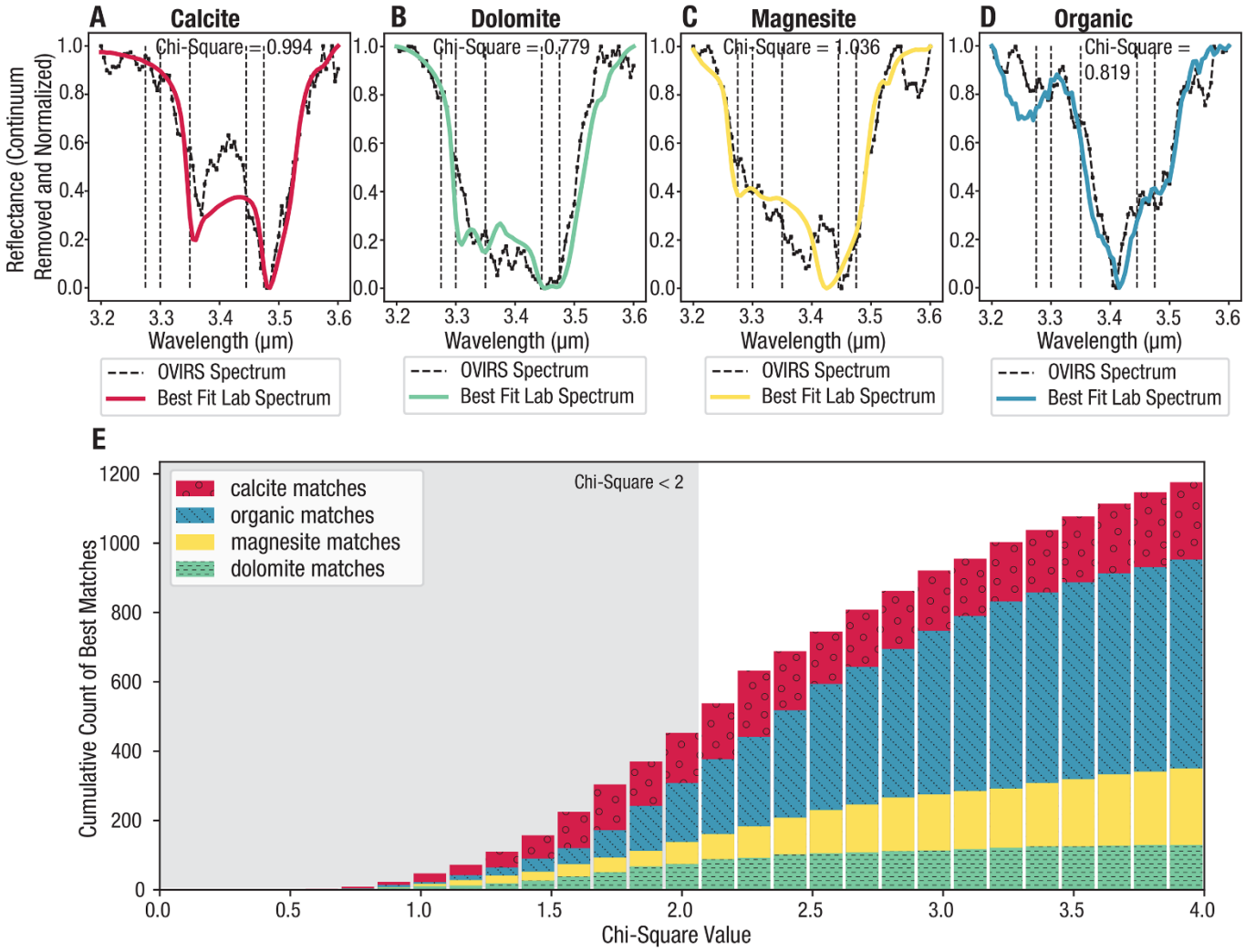

Fig. 2. Goodness of fit tests for laboratory carbonate spectra compared to OVIRS spectra. (**A** to **D**) Four different OVIRS spectra in the 3.4 μm region fit that are best fitted with laboratory spectra of calcite, dolomite, magnesite, and meteorite insoluble organic matter, respectively. (**E**) The cumulative count of all OVIRS spectra best fitted with either a calcite, dolomite, magnesite, or organic laboratory spectrum ordered by the chi-square value of the model. We discuss matches with chi-square < 2 (gray shaded region) in the text.

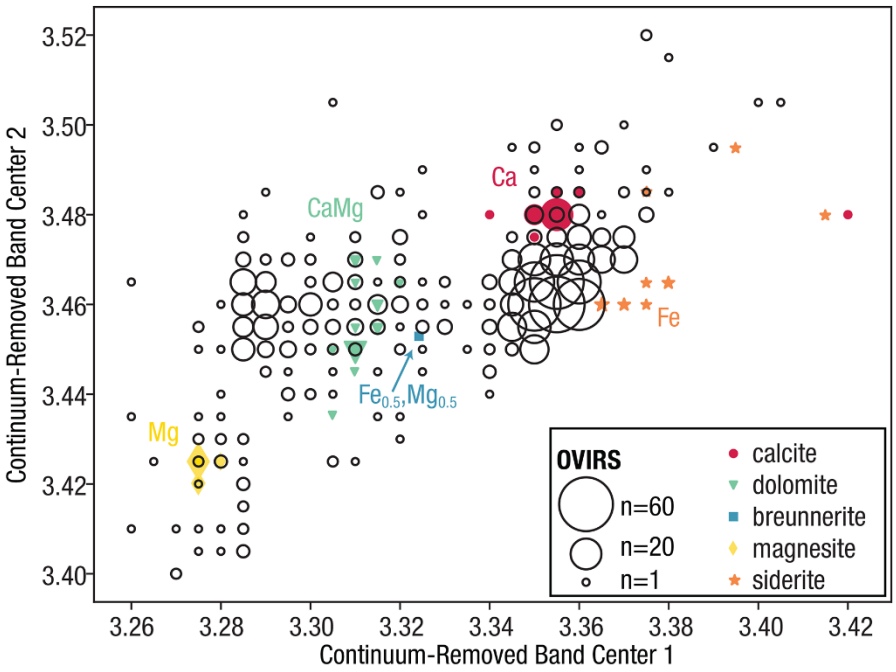

Fig. 3. Band minima positions of OVIRS signatures compared to laboratory spectra of carbonates. The positions of two carbonate band minima near 3.4 μm are plotted for Bennu (empty black circles), along with values for laboratory spectra (colored solid symbols, see legend and table S1). The OVIRS minima positions indicate a range of compositions on the surface. Circles are scaled to show the number of spectra represented, as indicated in the legend.

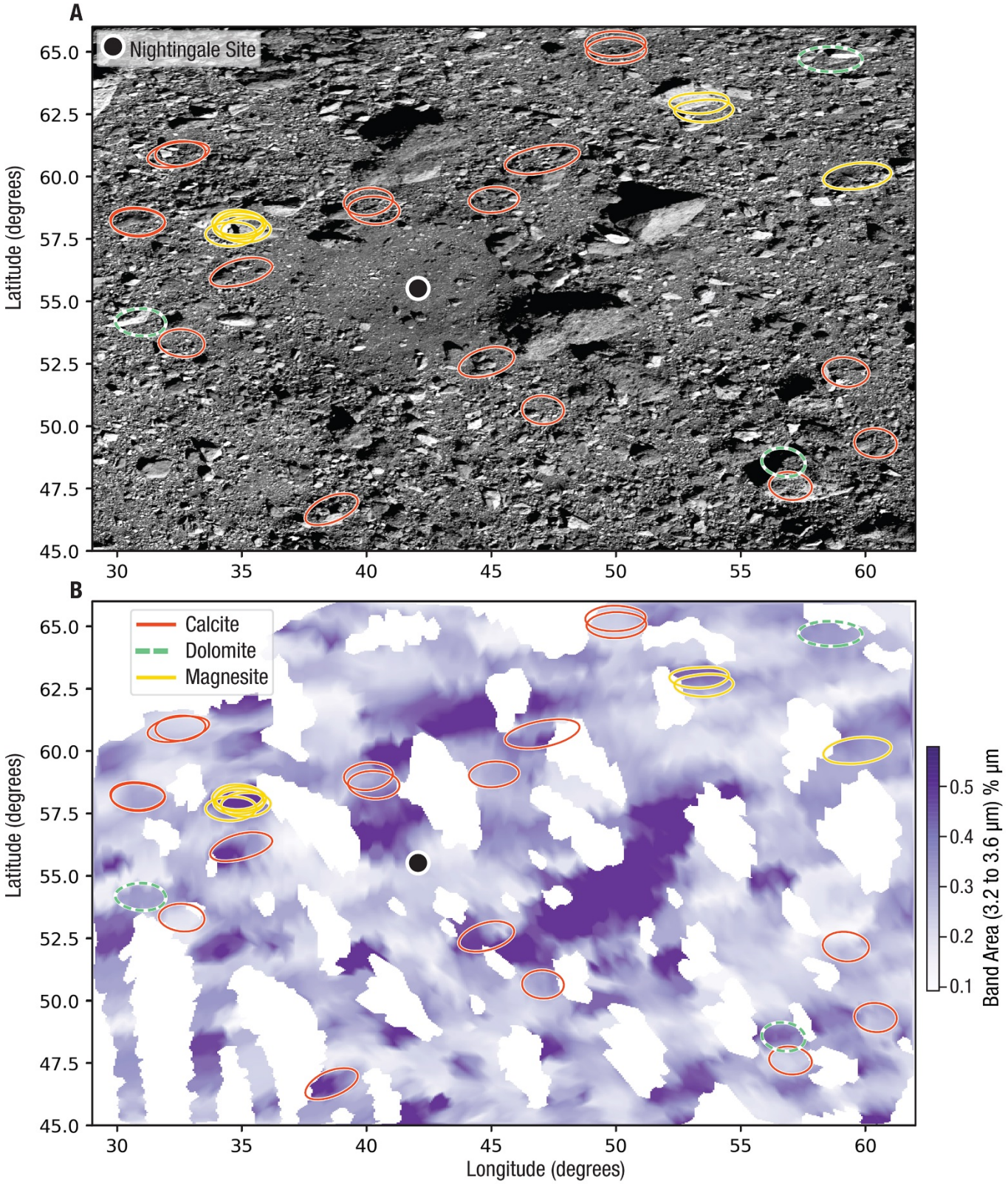

Fig. 4. Maps of carbonate-like spectral signatures at the Nightingale site and surrounding area. OVIRS footprints (colored ellipses, as indicated in the legend in (B)) of differing carbonate compositions are plotted over a panchromatic image (**A**) and over a map of band area from 3.2 to 3.6 µm (**B**). The band area does not distinguish between organics and carbonates but demonstrates overall contribution to the spectrum from carbon-bearing species. The Nightingale sample collection site is indicated with a black dot.

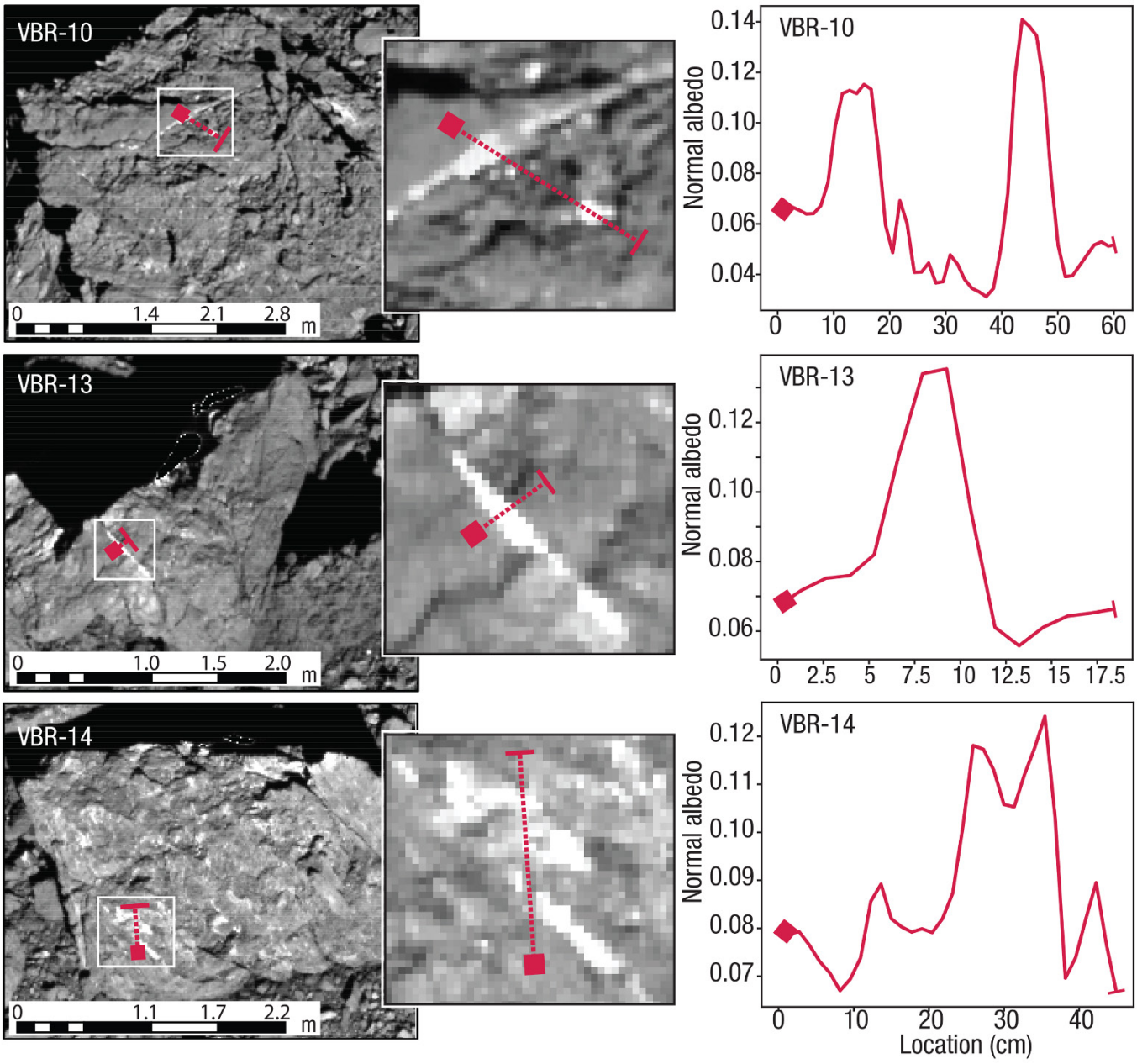

Fig. 5 Images and albedos of bright veins and irregularly shaped features on Bennu. Photometrically corrected PolyCam images (see text) of three boulders in the Nightingale region that host bright veins and irregular features. Transects across the bright features are indicated with red dotted lines, and normal albedos along the transects are plotted in panels X-Y. Albedos exceed 10%. VBR-10 is located at 51.56°N, 58.34°E; VBR-13 at 61.60°N, 50.57°E; and VBR-14 at 62.88°N, 71.55°E. Further images of the VBR-13 are shown in fig. S4.

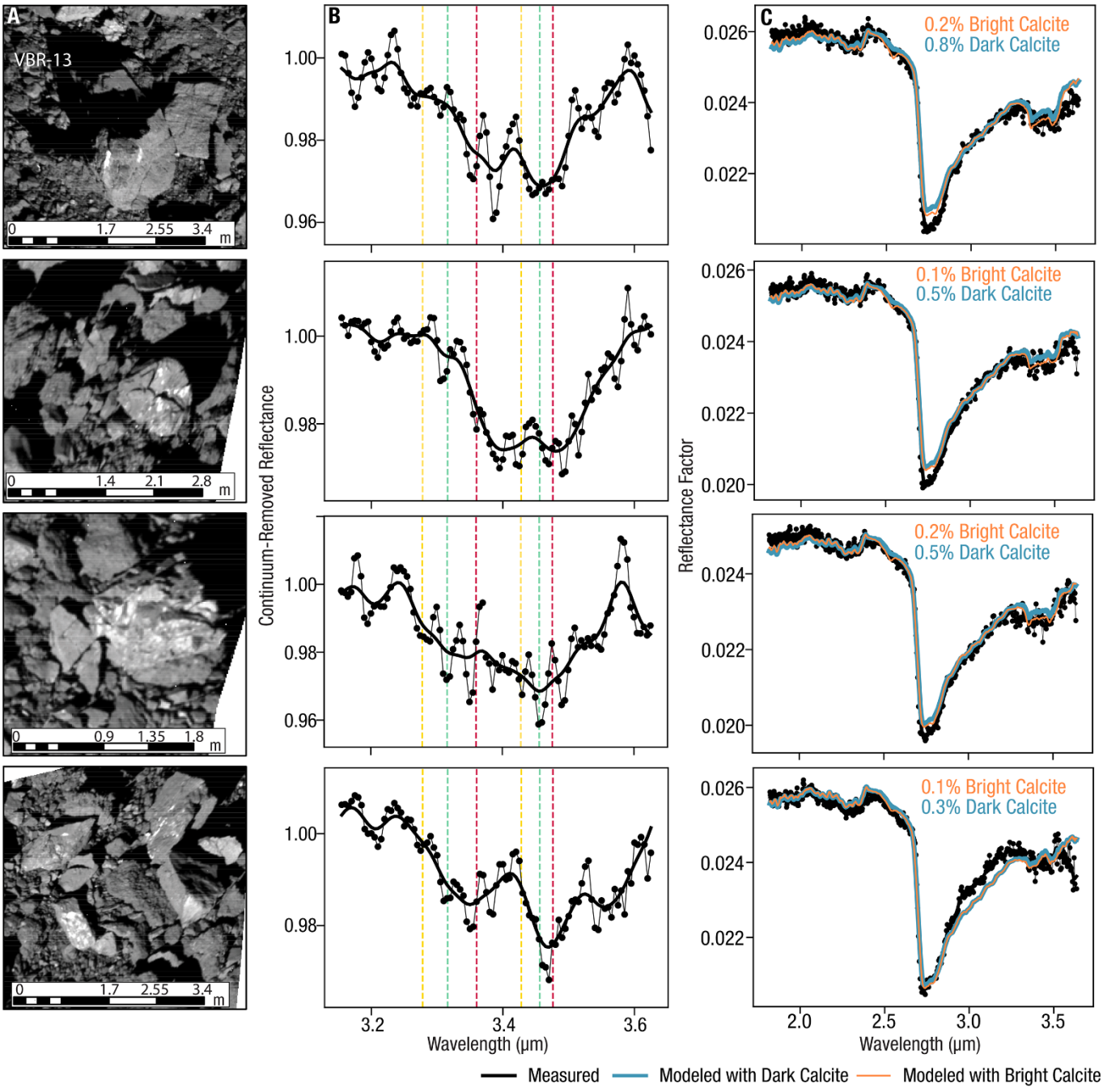

Fig. 6 Boulders with bright features and corresponding spectra. (A) PolyCam images of boulders with bright veins and irregularly shaped features in the Nightingale region. (B) OVIRS spectra of footprints that include each of these boulders have features near 3.4 μm that may be attributable to carbonates. Dashed vertical lines indicate the positions of band minima for calcite (red), dolomite/breunnerite (blue), and magnesite (yellow). (C) Linear mixture models (orange and blue lines) reproduce the observations (black data points) using a small fraction (<1%) of carbonate. The extent of the OVIRS footprints are shown in fig. S6 and spectral model endmembers are in fig. S7.

Bright carbonate veins on asteroid (101955) Bennu: Implications for aqueous alteration history

H. H. Kaplan, D. S. Lauretta, A. A. Simon, V. E. Hamilton, D. N. DellaGiustina, D. R. Golish, D. C. Reuter, C. A. Bennett, K. N. Burke, H. Campins, H. C. Connolly Jr., J. P. Dworkin, J. P. Emery, D. P. Glavin, T. D. Glotch, R. Hanna, K. Ishimaru, E. R. Jawin, T. J. McCoy, N. Porter, S. A. Sandford, S. Ferrone, B. E. Clark, J.-Y. Li, X.-D. Zou, M. G. Daly, O. S. Barnouin, J. A. Seabrook and H. L. Enos

published online October 8, 2020

Science (print ISSN 0036-8075; online ISSN 1095-9203) is published by the American Association for the Advancement of Science, 1200 New York Avenue NW, Washington, DC 20005. The title *Science* is a registered trademark of AAAS.